We are IntechOpen, the world's leading publisher of Open Access books Built by scientists, for scientists

4,800
Open access books available

122,000
International authors and editors

135M
Downloads

Our authors are among the

154
Countries delivered to

TOP 1%
most cited scientists

12.2%
Contributors from top 500 universities

WEB OF SCIENCE™

Selection of our books indexed in the Book Citation Index in Web of Science™ Core Collection (BKCI)

Interested in publishing with us?
Contact book.department@intechopen.com

Numbers displayed above are based on latest data collected.
For more information visit www.intechopen.com

6

Cervical Spine Anthropometric and Finite Element Biomechanical Analysis

Susan Hueston[1], Mbulelo Makola[1], Isaac Mabe[1] and Tarun Goswami[1,2]
[1]*Biomedical and Industrial Human Factors Engineering*
[2]*Department of Orthopedic Surgery, Sports Medicine and Rehabilitation*
United States of America

1. Introduction

A multidisciplinary approach to the study of the cervical spine is presented. The cervical spine provides higher levels of flexibility and motion as compared to the lumbar and thoracic spine regions. These characteristics can be attributed to the anatomy of the specific cervical vertebra. A statistical analysis of cervical vertebra anthropometry was performed in order to determine if significant relationships exist between vertebral features. The analysis was performed on a cohort of Chinese Singaporean cervical spines.
Mathematical analysis methods provide an extremely useful tool in the study of the cervical spine. Analyses can provide force displacement response characteristics of the cervical spine. Additionally, mathematical analysis methods can provide internal stress, and strain response characteristics for cervical vertebra and intervertebral discs. Mathematical analyses of the cervical spine require robust and accurate constitutive and geometric models. A review of cervical spine finite element modeling techniques and approaches is presented in order to help frame analysis and modeling best practices.
A finite element analysis study was performed focusing on vertebral endplate subsidence. Subsidence is a failure mechanism in which a vertebral endplate fails after implantation of an intra vertebral implant device. The effects of vertebral endplate morphology on stress response were analyzed in order to better understand indicators for subsidence.

1.1 Analysis of Chinese Singaporean cervical spine anthropometry

With respect to biomechanics it is important to understand the anatomy of the body. In this particular section the anatomy of the cervical spine will be presented, with investigation into the morphometry of the vertebra themselves. To accomplish this, an investigation on how the different dimensional anatomy of the cervical spine changes relates to each other will be presented.
To begin, a brief explanation of the anatomy of spine will be presented in order to aid in understanding of the anthropometry of the cervical spine. The spine consists of 5 sections: cervical, thoracic, lumbar, sacrum, and coccyx (from top to bottom) (Saladin and Miller, 2004). There are 33 vertebrae in the whole spine: 7 in the cervical spine which is located in the neck, 12 in the thoracic spine which is located in the chest, 5 in the lumbar spine which is located in the lower back, 5 in the sacrum that is located at the base of the spine, followed by the 4 small vertebrae in the coccyx (Saladin and Miller, 2004).

As stated previously there are 7 vertebrae in the cervical spine. The first two vertebrae are particularly unique and allow for movement of the head, the first is known as the Atlas (C1) and the second the Axis (C2) (Saladin and Miller, 2004). Because of their unique features analysis on correlations present in the dimensional anatomy was not completed. For the remaining 5 vertebrae from C3-C7 an investigation in the correlation in the dimensional anatomy was completed. The results of this investigation will allow for more accurate modeling of this region, in order to assist in the development of improved spinal implants as well as more efficient surgical device placement techniques. Additionally, these statistics will lead to a better understanding of cervical spine functionality and its susceptibility to failure. The different dimensional aspects that were analyzed were based on the anthropometric measurements completed from a published study by Tan on Chinese Singaporeans (Tan, Teo and Chua, 2004).

The present study involved the anthropometric measurements of linear, and angular aspects, as well as area. The linear measurements included: upper and lower end plate width (EPWu, and EPWl), upper and lower end plate depth (EPDu and EPDl), anterior and posterior vertebral body height (VBHa and VBHp), spinal canal width (SCW), spinal canal depth (SCD), left and right pedicle height (PDHl and PDHr), left and right pedicle width (PDWl and PDWr), spinous process length (SPL), and the transverse process width (TPW). The area measurements included: the upper and lower end plate area (EPAu and EPAl), spinal canal area (SCA), and the left and right pedicle area (PDAl and PDAr). Finally, the angular measurements included: upper and lower end plate transverse inclination (EPItu and EPItl), left and right pedicle sagittal inclination (PDIsl and PDIsr), and the left and right pedicle transverse inclination (PDItl and PDItr). Analysis was completed using the concepts of linear regression, ANOVA, and parameter estimation. Utilizing these results an investigation into any relationship that might be present between the previous anthropometric measurements was completed for each segment. As an example, a comparison between the EPWu of the C3 vertebra and the PDIsr of the C3 vertebra was analyzed to determine if there was any statistically significant relationship present (Tan, Teo and Chua, 2004).

Previous research, as discussed in this section, has been to provide quantitative measurements for the cervical spine. The purpose of the analysis completed was to develop any significant relationships present between the different anthropometrics of each vertebra. Of these significant relationships it was important to see why they were significant, which were significant in the opposite comparison (for example between EPWu vs. EPWl and EPWl vs. EPWu), and which were found in more than just one vertebral segment.

1.2 Materials & methods

To begin the analysis of the correlations present in the cervical spine anthropometrics, measurements were collected from Tan's study on Chinese Singaporeans. The linear, angular, and area measurements are depicted in Figure 1. In this analysis, a comparison of just one vertebral body's measurements was compared. A good example is comparing data from the C3 vertebra to other C3 vertebral data. These comparisons totaled approximately 600 for each vertebral body segment. The statistical analysis was completed using linear regression (including parameter estimation), and ANOVA with the use of SAS® 9.2 TS Level 2M0. A regression analysis is a statistical technique used to explore relationships that are present between two or more variables. In particular a linear regression analysis relates these various variables into a straight-line relationship where the slope and the y-intercept

of the line are the regression coefficients. Not all points will lie on this line, but a majority of the points will be within certain deviation of this line resulting in a model. For this particular study, a simple linear regression was used. It involves just one independent variable (x), also known as a regressor or predictor. With this linear regression analysis, parameter estimation was used. Parameter estimation is a technique of statistical inference, which is a way to make conclusions from random variation data. In this particular case, parameter estimation was used to find the y-intercept and the slope of the linear relationship between two anthropometric variables. ANOVA stands for Analysis of Variance, and can be used in order to test the significance of regression analysis. For the ANOVA, 95% confidence interval was used to test the significance between variables, while a 97.5% interval was used for the parameter estimation. Another test of significance was based off the R^2 value, which is also known as the correlation ratio. This correlation coefficient is the proportion of total variance of the dependent variable that is explained by the independent variable. Thus a higher value showing that the model is more accurate. In the case of the analysis described in this paper if the R^2 value was >0.6, the model was assumed to be a good fit (Montgomery and Peck, 1982; Gamst, Meyers and Guarino, 2008).
In the study completed by Tan on the Chinese Singaporeans, measurements of 10 cadaveric males were completed based on the measurements defined in Figure 1. The measurements mean and standard deviation found by Tan are displayed in Table's 1-3 where Table 1 displays the linear measurements, Table 2 lists the area measurements, and Table 3 illustrates the angular measurements that were taken in this study (Tan, Teo and Chua, 2004).

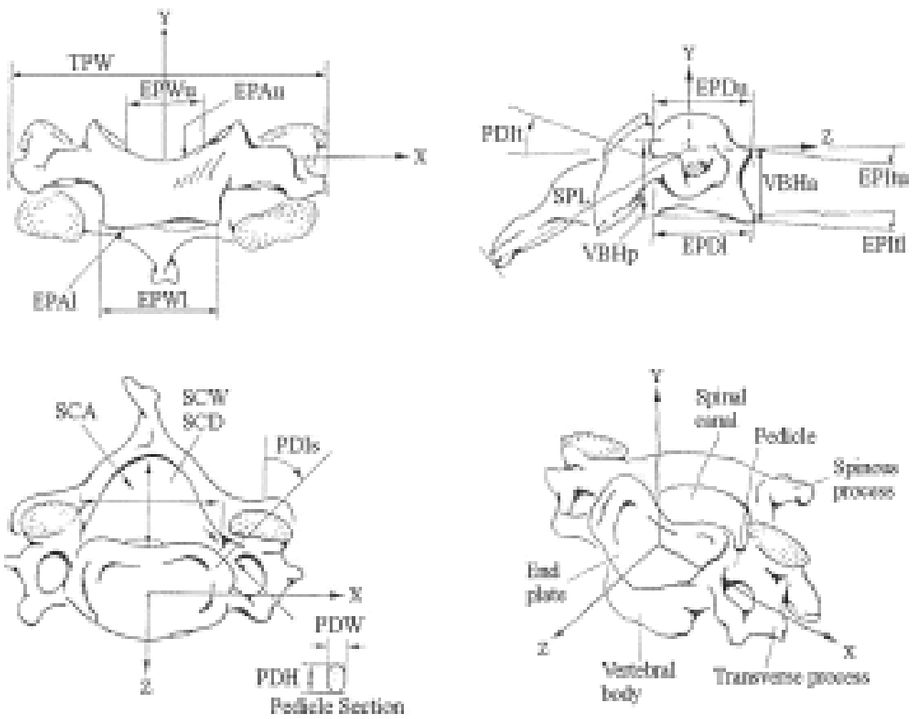

Fig. 1. Depiction of anthropometric measurements (Tan, Teo and Chua, 2004)

	C3		C4		C5		C6		C7	
	Mean	Std dev	Mean	Std dev	Mean	Std dev	Mean	Std dev	Mean	Std dev
EPWu	13.8	0.1	14.7	0.1	14.9	0.1	15.8	0.0	19.0	0.1
EPWl	14.3	0.1	15.0	0.1	15.9	0.1	19.5	0.2	20.3	0.2
EPDu	13.6	0.1	14.0	0.1	14.3	0.1	14.6	0.2	15.1	0.2
EPDl	15.1	0.2	15.2	0.4	15.1	0.3	15.7	0.3	15.6	0.3
VBHa	10.0	0.2	9.9	0.3	9.6	0.2	10.4	0.3	11.2	0.2
VBHp	11.2	0.1	11.3	0.2	11.3	0.1	11.3	0.2	11.8	0.3
SCW	19.2	0.4	19.3	0.5	20.3	0.4	20.6	0.4	19.7	0.4
SCD	10.3	0.3	10.3	0.3	10.3	0.3	10.3	0.3	11.0	0.2
PDHl	6.7	0.2	6.6	0.2	6.3	0.3	6.0	0.3	6.5	0.2
PDHr	6.8	0.2	6.7	0.2	5.9	0.2	6.0	0.1	6.1	0.1
PDWl	4.5	0.2	4.6	0.2	4.7	0.1	5.1	0.2	5.6	0.2
PDWr	4.4	0.2	4.5	0.2	4.9	0.2	5.4	0.2	5.7	0.2
SPL	25.6	0.5	30.3	0.4	33.6	1.0	40.5	1.5	46.9	1.1
TPW	41.4	0.8	44.9	0.8	47.6	1.0	48.4	0.9	53.8	1.0

Table 1. Linear Measurements from Tan study (mm) (Tan, Teo and Chua, 2004)

	C3		C4		C5		C6		C7	
	Mean	Std dev	Mean	Std dev	Mean	Std dev	Mean	Std dev	Mean	Std dev
EPAu	154.7	3.8	169.2	4.9	187.4	6.6	210.5	10.0	220.8	9.0
EPAl	216.8	10.1	241.5	10.6	286.4	10.3	316.3	7.4	340.0	10.3
SCA	149.7	9.0	159.9	8.4	166.8	8.0	163.7	10.2	167.5	6.7
PDAl	27.6	1.0	27.7	0.8	27.4	1.1	29.4	1.5	33.7	2.6
PDAr	28.5	1.0	28.8	1.0	28.5	1.1	33.0	1.3	32.1	1.6

Table 2. Surface Area measurements from Tan study (mm^2) (Tan, Teo and Chua, 2004)

Utilizing the mean and standard deviations from Tan's study, SAS® random number generation was used to create a normally distributed data set. From this random number generation, 100 observations were simulated in order to make the comparisons more robust. From this increase in sample size, linear regression analysis was completed simultaneously with the ANOVA. The results of this analysis are shown and discussed in succeeding paragraphs.

	C3		C4		C5		C6		C7	
	Mean	Std dev	Mean	Std dev	Mean	Std dev	Mean	Std dev	Mean	Std dev
EPItu	5.0	4.1	5.2	5.2	7.1	1.2	5.8	0.6	5.8	0.8
EPItl	3.3	0.5	3.5	0.7	2.7	0.3	4.2	0.4	5.1	0.5
PDIsl	-42.9	1.0	-44.0	1.3	-46.3	1.0	-41.9	1.6	-30.6	1.1
PDIsr	39.6	1.0	38.9	1.1	38.1	1.6	38.5	2.3	30.3	0.9
PDItl	-4.8	1.0	-3.2	0.7	2.6	0.7	4.8	1.0	5.8	0.7
PDItr	-6.5	1.0	-5.4	1.1	4.9	1.0	6.0	1.3	3.1	0.7

Table 3. Angular measurements from Tan study (degrees) (Tan, Teo and Chua, 2004)

1.3 Analysis

To find correlations present in the anthropometrics of the vertebral bodies in the cervical spine, statistical analysis was completed on each vertebral segment from C3 to C7. Initially, investigation into the C3 vertebra was completed, starting with the linear measurements. As an example, the C3_EPWu was compared to all 24 other measured parameters of the C3 vertebra. This resulted in 14 linear measurements compared to 24 other measurement parameters for the C3 vertebra, resulting in a total of 336 comparisons.

From analysis of the C3 linear measurements it was found that there were 8 significant correlations present among all 336 comparisons. These results are shown in Table 4. The dependent variables are listed first with the regressor/independent showing second. The first case illustrates that the C3_PDWr is the dependent variable and C3_VBHp is the regressor or independent variable. From analysis of the area measurements of the C3 vertebra, only one significant correlation was present among 120 comparisons (Table 5). Finally when comparing the angular measurements of the C3 vertebra, it was found that there were 2 significant correlations among a total of 144 comparisons (Table 6).

The examination of the other vertebral segments, from C4 to C7, was accomplished in a similar fashion. Analysis of the C4 vertebra resulted in extensively more significant relationships than were found in C3 with a total of 23 significant correlations.

Comparisons of the linear measurements of the C4 vertebra yielded 12 strong relationships, and these results are shown in Table 7. From investigation into the area measurements of the C4 vertebra, it was found that there were five comparisons of anthropometrics that had a considerable link among 120 comparisons (shown in Table 8). Finally when comparing the angular measurements of the C4 vertebra to the other 24 measurements (include all three forms of linear, area, and angular), there were 6 strong relationships found from the 144 total comparisons. All of the significant correlations of the angular measurements can be found in Table 9.

In completing the investigation into the C5 vertebra, it was again found to have increasingly more relationships, with a total of 40 strong correlations. The comparisons of the linear measurements of the C5 vertebra to the rest of the anthropometric measurements resulted in the most relationships; these are displayed in Tables 10 and 11. Of these comparisons there were 21 relationships found in the C5 vertebral body anthropometrics. With the investigation into the area measurements of the C5 vertebra, it was found that there were 10 significant correlations from a total of 120 comparisons completed. Finally in investigating

	ANOVA	Parameter Estimates		Y-intercept	Slope
	P	P (y-intercept)	P (regressor/ independent)		
PDWr vs. VBHp	0.0424	<0.0001	0.0424	8.34113	-0.3523
	Significant	Significant	Not Significant		
PDWr vs. SCW	0.0166	0.0043	0.0166	2.39346	0.10409
	Significant	Significant	Significant		
SCD vs. PDHl	0.0085	<0.0001	0.0085	12.88191	-0.3927
	Significant	Significant	Significant		
TPW vs. EPItl	0.0324	<0.0001	0.0324	40.20551	0.3705
	Significant	Significant	Not Significant		
TPW vs. PDIsr	0.0068	<0.0001	0.0068	50.21888	-0.22291
	Significant	Significant	Significant		
VBHa vs. EPDu	0.0062	<0.0001	0.0062	17.51686	-0.55302
	Significant	Significant	Significant		
VBHa vs. PDAl	0.0149	<0.0001	0.0149	11.47438	-0.05326
	Significant	Significant	Significant		
VBHp vs. PDWr	0.0024	<0.0001	0.0024	10.52205	0.15663
	Significant	Significant	Significant		

Table 4. C3 Linear measurements

	ANOVA	Parameter Estimates		Y-intercept	Slope
	P	P (y-intercept)	P (regressor/ independent)		
PDAl vs. EPAu	0.0061	0.0024	0.0061	14.53586	0.08468
	Significant	Significant	Significant		

Table 5. C3 Area measurements

	ANOVA	Parameter Estimates		Y-intercept	Slope
	P	P (y-intercept)	P (regressor/ independent)		
EPItl vs. EPWu	0.0124	0.0413	0.0124	15.04667	-0.85215
	Significant	Not Significant	Significant		
EPItu vs. EPDu	0.0419	0.0355	0.0419	33.19859	-2.07824
	Significant	Not Significant	Not Significant		

Table 6. C3 Angular measurements

	ANOVA	Parameter Estimates			
	P	P (y-intercept)	P (regressor/ independent)	Y-intercept	Slope
EPDl vs. SPL	0.0245	0.0006	0.0245	9.21517	0.19714
	Significant	Significant	Significant		
EPDu vs. EPWu	0.02	<0.0001	0.02	10.32639	0.24868
	Significant	Significant	Significant		
EPWl vs. PDItr	0.0326	<0.0001	0.0326	15.10987	0.01808
	Significant	Significant	Not Significant		
EPWu vs. PDWr	0.0248	<0.0001	0.0248	15.14845	-0.10029
	Significant	Significant	Significant		
PDHr vs. EPDl	0.0303	<0.0001	0.0303	8.23208	-0.10071
	Significant	Significant	Not Significant		
PDWl vs. EPDl	0.0076	0.0003	0.0076	2.66256	0.12866
	Significant	Significant	Significant		
SCD vs. EPItu	0.0207	<0.0001	0.0207	10.30332	0.01353
	Significant	Significant	Significant		
SCW vs. VBHa	0.0056	<0.0001	0.0056	13.58683	0.56164
	Significant	Significant	Significant		
SCW vs. TPW	0.0323	<0.0001	0.0323	23.82069	-0.11106
	Significant	Significant	Not Significant		
TPW vs. EPDu	0.0108	<0.0001	0.0108	68.19806	-1.95975
	Significant	Significant	Significant		
TPW vs. SCW	0.0323	<0.0001	0.0323	49.4967	-0.41322
	Significant	Significant	Not Significant		
VBHp vs. PDAl	0.0348	<0.0001	0.0348	9.47331	0.06488
	Significant	Significant	Not Significant		

Table 7. C4 Linear Measurements

the relationships present in the C5 vertebra angular measurements and the other anthropometric measurements, 9 significant correlations were found. The strong relationships that were present in the C5 vertebra's angular measurements are displayed in Table 13.

	ANOVA	Parameter Estimates			
	P	P (y-intercept)	P (regressor/ independent)	Y-intercept	Slope
EPAu vs. EPWu	0.0104	0.66909	0.0104	-34.27382	13.8368
	Significant	Not Significant	Significant		
EPAu vs. VBHa	0.0219	<0.0001	0.0219	204.59603	-3.58479
	Significant	Significant	Significant		
EPAu vs. PDWl	0.0288	<0.0001	0.0288	143.55496	5.63237
	Significant	Significant	Not Significant		
EPAu vs. PDItl	0.0046	<0.0001	0.0046	161.94009	-2.29035
	Significant	Significant	Significant		
SCA vs. SCW	0.0066	0.0093	0.0066	78.19896	4.24208
	Significant	Significant	Significant		

Table 8. C4 Area Measurements

	ANOVA	Parameter Estimates			
	P	P (y-intercept)	P (regressor/ independent)	Y-intercept	Slope
EPItl vs. EPDl	0.0191	0.3069	0.0191	-2.63366	0.40237
	Significant	Not Significant	Significant		
EPItl vs. VBHp	0.0064	0.0781	0.0064	-6.16074	0.8523
	Significant	Not Significant	Significant		
EPItl vs. SCW	0.0345	0.4489	0.0345	-1.91019	0.27823
	Significant	Not Significant	Not Significant		
PDIsl vs. SCW	0.0437	<0.0001	0.0437	-55.42757	0.59539
	Significant	Significant	Not Significant		
PDIsl vs. EPItl	0.0178	<0.0001	0.0178	-42.30098	-0.46784
	Significant	Significant	Significant		
PDIsr vs. VBHp	0.0076	<0.0001	0.0076	24.45626	1.27529
	Significant	Significant	Significant		

Table 9. C4 Angular Measurements

	ANOVA	Parameter Estimates		Y-intercept	Slope
	P	P (y-intercept)	P (regressor/ independent)		
EPDl vs SCW	0.0272	<0.0001	0.0272	11.78609	0.1654
	Significant	Significant	Not Significant		
EPDl vs SCA	0.0014	<0.0001	0.0014	17.20746	-0.01233
	Significant	Significant	Significant		
EPDu vs SCA	0.0415	<0.0001	0.0415	13.85796	0.0026
	Significant	Significant	Not Significant		
EPDu vs PDItl	0.0405	<0.0001	0.0405	14.22233	0.02818
	Significant	Significant	Not Significant		
EPWl vs PDWr	0.0394	<0.0001	0.0394	15.30981	0.11428
	Significant	Significant	Not Significant		
EPWu vs VBHa	0.0353	<0.0001	0.0353	15.79112	-0.09338
	Significant	Significant	Not Significant		
EPWu vs EPAu	0.0465	<0.0001	0.0465	14.35019	0.00291
	Significant	Significant	Not Significant		
PDHl vs PDWl	0.0207	0.0426	0.0207	2.90559	0.70698
	Significant	Not Significant	Significant		
PDHl vs PDIsr	0.0488	<0.0001	0.0488	7.36108	-0.02888
	Significant	Significant	Not Significant		
PDWl vs PDHl	0.0207	<0.0001	0.0207	4.23321	0.0756
	Significant	Significant	Significant		
PDWl vs PDAr	0.0189	<0.0001	0.0189	5.30502	-0.02109
	Significant	Significant	Significant		
PDWr vs EPWl	0.0394	0.722	0.0394	-1.01063	0.37265
	Significant	Not Significant	Not Significant		
PDWr vs EPItu	0.026	<0.0001	0.026	4.64358	0.03596
	Significant	Significant	Not Significant		
PDWr vs PDItl	0.0213	<0.0001	0.0213	4.7488	0.06132
	Significant	Significant	Significant		
SCD vs VBHp	0.033	0.4903	0.033	2.50118	0.69204
	Significant	Not Significant	Not Significant		
SCD vs EPAu	0.0167	<0.0001	0.0167	12.49697	-0.01164
	Significant	Significant	Significant		
SCW vs EPDl	0.0272	<0.0001	0.0272	15.81713	0.29501
	Significant	Significant	Not Significant		
SPL vs PDItr	0.0117	<0.0001	0.0117	34.72062	-0.23666
	Significant	Significant	Significant		
VBHa vs EPWu	0.0353	<0.0001	0.0353	16.67726	-0.47571
	Significant	Significant	Not Significant		

Table 10. C5 Linear Measurements (Part 1)

	ANOVA	Parameter Estimates		Y-intercept	Slope
	P	P (y-intercept)	P (regressor/ independent)		
VBHp vs SCD	0.033	<0.0001	0.033	10.60996	0.06583
	Significant	Significant	Not Significant		
VBHp vs PDAl	0.0163	<0.0001	0.0163	10.72456	0.0205
	Significant	Significant	Significant		

Table 11. C5 Linear Measurements (Part 2)

	ANOVA	Parameter Estimates		Y-intercept	Slope
	P	P (y-intercept)	P (regressor/ independent)		
EPAl vs. EPDl	0.0126	<0.0001	0.0126	418.92547	-8.70812
	Significant	Significant	Significant		
EPAu vs. EPDl	0.0356	0.0001	0.0356	122.32733	4.3305
	Significant	Significant	Not Significant		
EPAu vs. SCD	0.0317	<0.0001	0.0317	21.37129	2.08213
	Significant	Significant	Not Significant		
EPAu vs. PDAl	0.0282	<0.0001	0.0282	156.25957	1.14813
	Significant	Significant	Not Significant		
PDAl vs. VBHp	0.0163	0.7504	0.0163	-4.13231	2.80491
	Significant	Not Significant	Significant		
PDAr vs. PDWl	0.0189	<0.0001	0.0189	40.73714	-2.60613
	Significant	Significant	Significant		
PDAr vs. PDIsr	0.0178	<0.0001	0.0178	23.56205	0.12563
	Significant	Significant	Significant		
PDAr vs. PDItr	0.0356	<0.0001	0.0356	29.53373	-0.21079
	Significant	Significant	Not Significant		
SCA vs. EPDu	0.0415	0.5788	0.0415	-61.91478	16.06134
	Significant	Not Significant	Not Significant		
SCA vs. EPDl	0.0014	<0.0001	0.0014	290.35634	-8.10387
	Significant	Significant	Significant		

Table 12. C5 Area Measurements

	ANOVA	Parameter Estimates		Y-intercept	Slope
	P	P (y-intercept)	P (regressor/ independent)		
EPItu vs. PDWr	0.026	0.8775	0.026	0.46263	1.37892
	Significant	Not Significant	Not Significant		
PDIsl vs. PDItl	0.0488	<0.0001	0.0488	-45.50392	-0.24512
	Significant	Significant	Not Significant		
PDIsr vs. PDHl	0.0488	<0.0001	0.0488	47.54716	-1.35216
	Significant	Significant	Not Significant		
PDIsr vs. PDAr	0.0178	<0.0001	0.0178	26.44105	0.44528
	Significant	Significant	Significant		
PDItl vs. EPDu	0.0405	0.0701	0.0405	-18.8499	1.4951
	Significant	Not Significant	Not Significant		
PDItl vs. PDWr	0.0213	0.3461	0.0213	-1.71369	0.86345
	Significant	Not Significant	Significant		
PDItl vs. PDIsl	0.0488	0.1931	0.0488	-4.82456	-0.15925
	Significant	Not Significant	Not Significant		
PDItr vs. SPL	0.0117	0.0001	0.0117	13.95113	-0.26654
	Significant	Significant	Significant		
PDItr vs. PDAr	0.0356	0.0002	0.0356	10.99851	-0.21019
	Significant	Significant	Not Significant		

Table 13. C5 Angular Measurements

In the analysis of the C6 vertebra 22 strong relationships, less than what was seen in the C5 and C4 vertebra but more than what was seen in the C3 vertebra. Investigation of the C6 linear measurements and comparisons between the other anthropometric measurements discovered 15 significant comparisons out of a total of 336 comparisons completed. These results are shown in Table 14. Exploration into the relationships present in the C6 vertebra area measurements in comparison to the other anthropometrics, showed that there were two significant correlations present (shown in Table 15). Finally analysis of the C6 vertebra and the angular measurements comparisons to the other anthropometrics, found there to be 5 strong relationships from a total of 144 comparisons made (Table 16).

In the analysis of the C7 vertebra there were 34 significant relationships found. Thus finding that the C7 vertebra has more correlations present than all the other vertebra's except for C5. Investigation of the C7 linear measurements and comparing them with the other anthropometrics discovered 18 comparisons with strong relationships from 336 comparisons completed. The result of this is displayed in Tables 17 and 18. Exploration into the relationships present in the C7 vertebra area measurements divulged that there were five significant correlations present (shown in Table 19). Finally analysis of the C7's angular measurements found 11 strong relationships out of 144 comparisons made (Table 20).

1.4 Discussion

Through investigation into correlations that may be present within the anthropometric data of each vertebra, there were a total of 130 significant relationships discovered:

- 11 in the C3 vertebra
- 23 in the C4 vertebra
- 40 in the C5 vertebra
- 22 in the C6 vertebra
- 34 in the C7 vertebra.

Some of these relationships were physiologically reconcilable, in particular for the C3 vertebral segment the upper endplate transverse inclination and the upper endplate depth (EPItu & EPDu). From looking at Figure 1 it can be seen how the EPItu would possibly increase in the same way as the EPDu increases based on a person's stature.

As for the C4 vertebral segment the correlations that make the most sense are the upper endplate area vs. the upper endplate width (EPAu vs. EPWu), the upper endplate depth vs. the upper endplate width (EPDu vs. EPWu), and the lower endplate transverse inclination vs. the lower endplate depth (EPItl vs. EPDl). In the study completed by Panjabi they found that modeling the area of the endplates, spinal canal, and pedicles as ellipses was "justified" (Liu, Clark and Krieger, 1986). So when looking at the case of the EPAu and the EPWu, this relationship can be explained by the area of an ellipse. Since the area of an ellipse is Area= πab where a and b are depicted in Figure 2 as the radius. In the same aspect since a radius of an ellipse is the diameter divided by 2 ($a = \frac{a'}{2} or\, b = \frac{b'}{2}$) then the area can also equate to Area= $\pi\left(\frac{a'}{2}\right)\left(\frac{b'}{2}\right)$, where a′ and b′ are depicted in Figure 2 as the diameters. In this case EPWu would be b′ and the area would be EPAu. So as the diameter EPWu increases so does the area EPAu.

As for the relationship found between the EPDu and the EPWu, the same argument may be placed that the depth of the end plate could be seen as the diameter as well, as shown here:

$$Area = \pi\left(\frac{a'}{2}\right)\left(\frac{b'}{2}\right)$$

$$EPAu = \pi\left(\frac{EPDu}{2}\right)\left(\frac{EPWu}{2}\right)$$

In the case for the relationship between the EPItl and the EPDl, the same statement as stated for the C3 vertebra in the case of the EPItu and the EPDu can be stated.

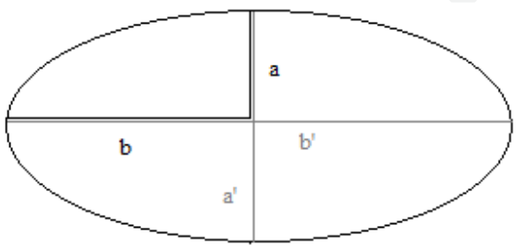

Fig. 2. Diagram of an ellipse to describe the area of an ellipse, where a and b are the radius and a′ and b′ are the diameters

	ANOVA	Parameter Estimates		Y-intercept	Slope
	P	P (y-intercept)	P (regressor/ independent)		
EPDl vs. EPWl	0.03	0.0158	0.03	8.2642	0.37956
	Significant	Significant	Not Significant		
EPDu vs. PDWl	0.0048	<0.0001	0.0048	13.16703	0.26669
	Significant	Significant	Significant		
EPWu vs. PDWr	0.0155	<0.0001	0.0155	15.80078	-0.0001436
	Significant	Significant	Significant		
PDHl vs. EPDu	0.0425	0.3398	0.0425	1.91753	0.28098
	Significant	Not Significant	Not Significant		
PDHr vs. EPDu	0.0181	<0.0001	0.0181	7.42367	-0.09719
	Significant	Significant	Significant		
PDHr vs. PDItl	0.0166	<0.0001	0.0166	5.88497	0.02407
	Significant	Significant	Significant		
SCD vs. EPDl	0.0198	<0.0001	0.0198	7.52521	0.1789
	Significant	Significant	Significant		
SCD vs. EPAl	0.0127	<0.0001	0.0127	7.53602	0.00885
	Significant	Significant	Significant		
SPL vs. PDItr	0.0405	<0.0001	0.0405	41.94107	-0.2777
	Significant	Significant	Not Significant		
TPW vs. PDItr	0.0321	<0.0001	0.0321	47.35028	0.16667
	Significant	Significant	Not Significant		
VBHa vs. EPDl	0.0179	<0.0001	0.0179	7.27923	0.19901
	Significant	Significant	Significant		
VBHa vs. VBHp	0.0283	0.0025	0.0283	6.0541	0.38446
	Significant	Significant	Not Significant		
VBHa vs. SCW	0.0451	<0.0001	0.0451	7.66983	0.13244
	Significant	Significant	Not Significant		
VBHa vs. EPAu	0.0046	<0.0001	0.0046	12.01819	-0.00769
	Significant	Significant	Significant		
VBHp vs. VBHa	0.0283	<0.0001	0.0283	10.00304	0.12525
	Significant	Significant	Not Significant		

Table 14. C6 Linear Measurements

For the C5 vertebral segment, the associations found that were physiologically reconcilable were in:

- The lower endplate area vs. the lower endplate depth (EPAl vs. EPDl)
- The upper endplate area vs. the lower endplate depth (EPAu vs. EPDl)
- The pedicle height on the left side vs. the pedicle width on the left side (PDHl vs. PDWl)
- The pedicle sagittal inclination on the left side vs. the pedicle transverse inclination on the left side (PDIsl vs. PDItl)
- The pedicle transverse inclination on the left side vs. the pedicle sagittal inclination on the left side (PDItl vs. PDIsl)
- The pedicle width on the left side vs. the pedicle height on the left side (PDWl vs. PDHl)

As for the correlations in the EPAl vs. EPDl, EPAu vs. EPDl, PDHl vs. PDWl, and PDWl vs. PDHl these can be explained in the same aspect as the relationships found in the C4 vertebra; with comparison of the area of an ellipse and the diameter of an ellipse, along with the diameter to diameter comparison of a ellipse. In the cases of the relationships present in the sagittal inclination and the transverse inclination, if looking at Figure 1 it can be seen how as one increases the other may increase.

In the C6 vertebral segment the relationships that were the most physiologically reconcilable are the lower endplate depth and the lower endplate width (EPDl and EPWl), this type of relationship was explained previously with the examination into the C4 vertebra and relationship present in diameter to diameter comparison of an ellipse. As for the relationship found between the anterior vertebral body height and the posterior vertebral body height (VBHa and VBHp), again if looking at Figure 1 it can be seen that if the height increases in either the anterior or posterior location of the vertebral body that there should be an increase in the former as well.

	ANOVA	Parameter Estimates		Y-intercept	Slope
	P	P (y-intercept)	P (regressor/ independent)		
EPAl vs. TPW	0.0289	<0.0001	0.0289	407.91242	-1.90819
	Significant	Significant	Not Significant		
PDAl vs. EPDl	0.0168	<0.0001	0.0168	44.79661	-0.9836
	Significant	Significant	Significant		

Table 15. C6 Area Measurements

Unlike the other vertebras, the C7 vertebra had no obvious relationships that were physiologically reconcilable. As for the other relationships found that were not described they were not physiological reconcilable. But they will help in further research as discussed earlier since they were found to be statistically significant.

It is of interest to investigate the findings further. In particular any relationships that was present and also present in the opposite comparison. As an example if a link was found between upper endplate width vs. the lower endplate width (EPWu vs. EPWl) and also a link between the lower endplate width vs. the upper endplate width (EPWl vs. EPWu).

	ANOVA	Parameter Estimates		Y-intercept	Slope
	P	P (y-intercept)	P (regressor/ independent)		
PDIsr vs. PDItl	0.0332	<0.0001	0.0332	41.66266	-0.60909
	Significant	Significant	Not Significant		
PDItl vs. PDHr	0.0166	0.1125	0.0166	-9.36715	2.3752
	Significant	Not Significant	Significant		
PDItl vs. PDIsr	0.0332	<0.0001	0.0332	7.77712	-0.07463
	Significant	Significant	Not Significant		
PDItr vs. SPL	0.0405	<0.0001	0.0405	12.26138	-0.1517
	Significant	Significant	Not Significant		
PDItr vs. TPW	0.0321	0.2446	0.0321	-7.19097	0.27594
	Significant	Not Significant	Not Significant		

Table 16. C6 Angular Measurements

For the C3 vertebra there was only one case that this was seen in:

- The pedicle width on the right side vs. the posterior vertebral body height and the posterior vertebral body height vs. the pedicle width on the right side (PDWr vs. VBHp and VBHp vs. PDWr).
- In the C4 vertebra there was also one case of this same type of connection which was seen in:
- The spinal canal width and the transverse process width (SCW and TPW).
- The C5 vertebra had increasingly more connections of this type and included the following:
- The lower endplate depth and the spinal canal width (EPDl and SCW)
- The lower endplate depth and the spinal canal area (EPDl and SCA)
- The upper endplate depth and the spinal canal area (EPDu and SCA)
- The upper endplate depth and the pedicle transverse inclination (EPDu and PDItl)
- The lower endplate width and the pedicle width on the right side (EPWl and PDWr)
- The upper endplate width and the anterior vertebral body height (EPWu and VBHa)
- The pedicle height on the left side and the pedicle width on the left side (PDHl and PDWl)
- The pedicle height on the left side and the pedicle sagittal inclination on the right side (PDHl and PDIsr)
- The pedicle width on the left side and the pedicle area on the right side (PDWl and PDAr)
- The pedicle width on the right side and the upper endplate transverse inclination (PDWr and EPItu)
- The pedicle width on the right side and the pedicle transverse inclination on the left side (PDWr and PDItl)
- The spinal canal depth and the posterior vertebral body height (SCD and VBHp)

- The spinal canal depth and the upper endplate area (SCD and EPAu)
- The spinous process length and the pedicle transverse inclination on the right side (SPL and PDItr)
- The posterior vertebral body height and the pedicle area on the left side (VBHp and PDAl)
- The pedicle area on the right side and the pedicle sagittal inclination on the right side (PDAr and PDIsr)
- The pedicle sagittal inclination on the left side and the pedicle transverse inclination on the left side (PDIsl and PDItl).

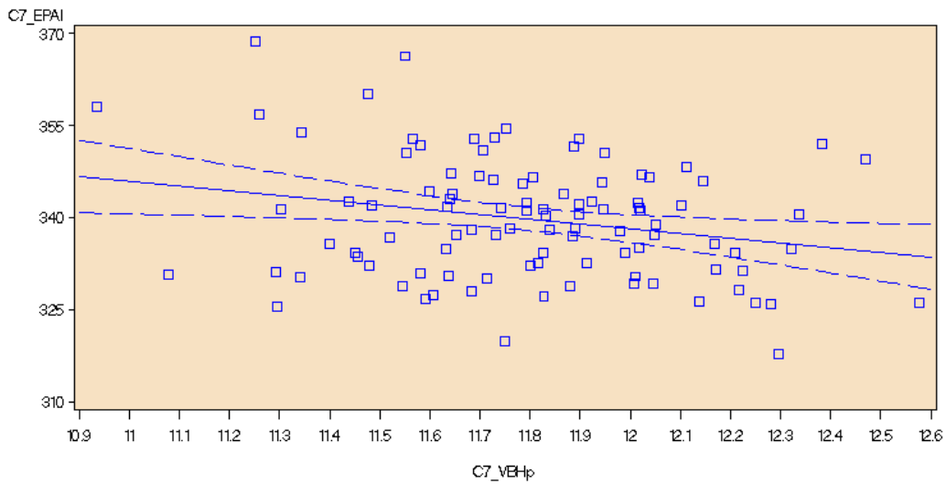

Fig. 3. Scatter plot of C7_EPAl vs. C7_VBHp

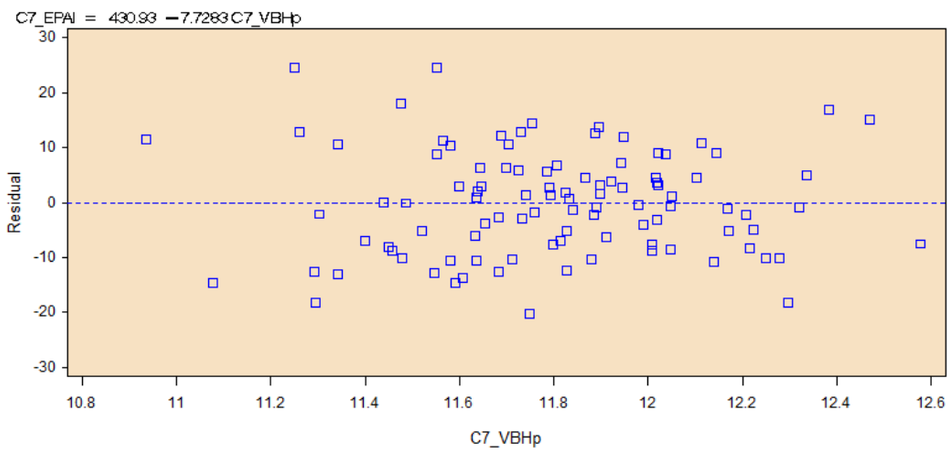

Fig. 4. Residual vs. C7_VBHp

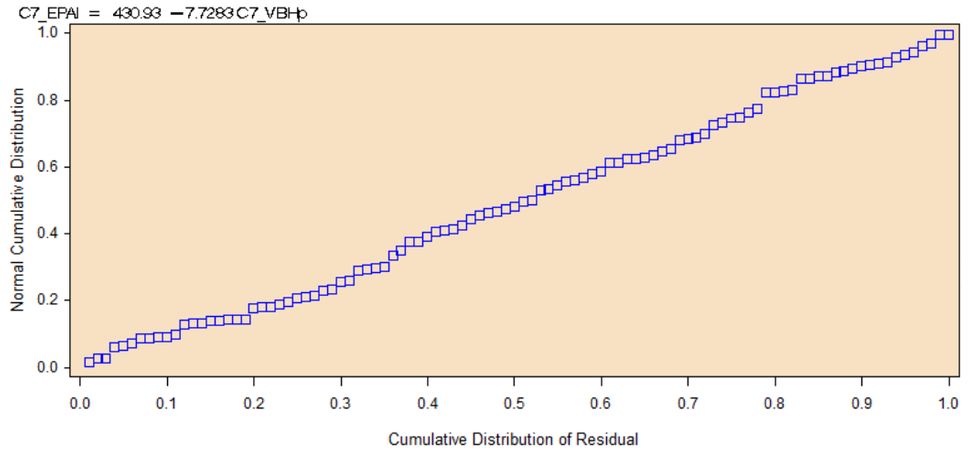

Fig. 5. Normal Cumulative Distribution vs. Cumulative Distribution of Residual

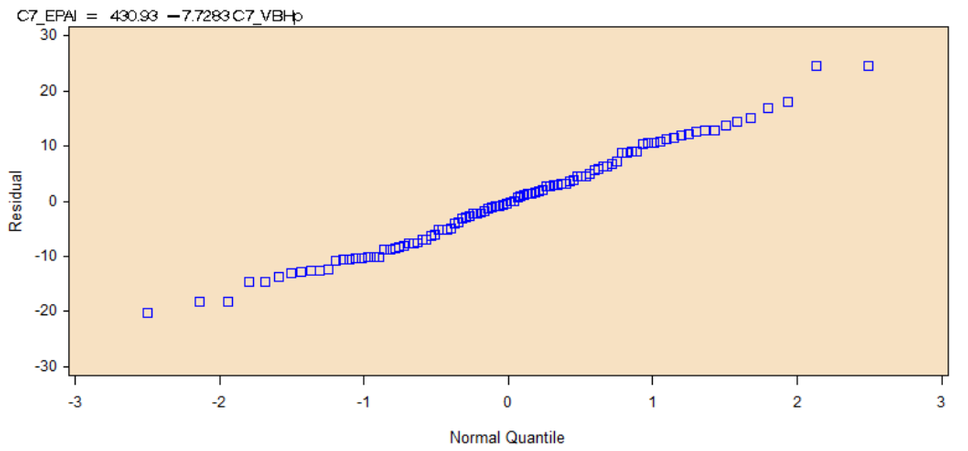

Fig. 6. Residual vs. Normal Quantile

In the C6 vertebra there were five connections of this type which were:

- The pedicle height on the right side and the pedicle transverse inclination on the left side (PDHr and PDItl)
- The spinous process length and the pedicle transverse inclination on the right side (SPL and PDItr)
- The transverse process width and the pedicle transverse inclination on the right side (TPW and PDItr)
- The anterior vertebral body height and the posterior vertebral body height (VBHa and VBHp)
- The pedicle sagittal inclination on the right side and the pedicle transverse inclination on the left side (PDIsr and PDItl).
- Finally for the C7 vertebra there were fifteen connections of this type which included:
- The lower endplate area and the upper endplate depth (EPAl and EPDu)
- The lower endplate area and the posterior vertebral body height (EPAl and VBHp)
- The upper endplate area and the lower endplate depth (EPAu and EPDl)

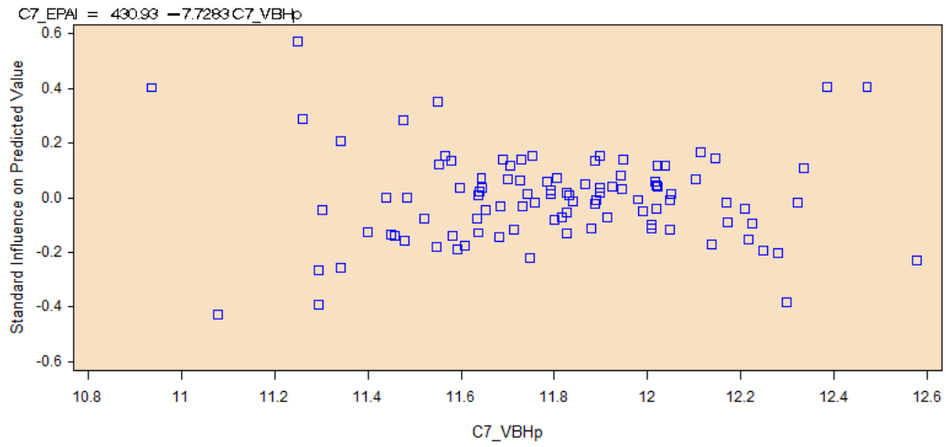

Fig. 7. Standard Influence on Predicted Value vs. C7_VBHP

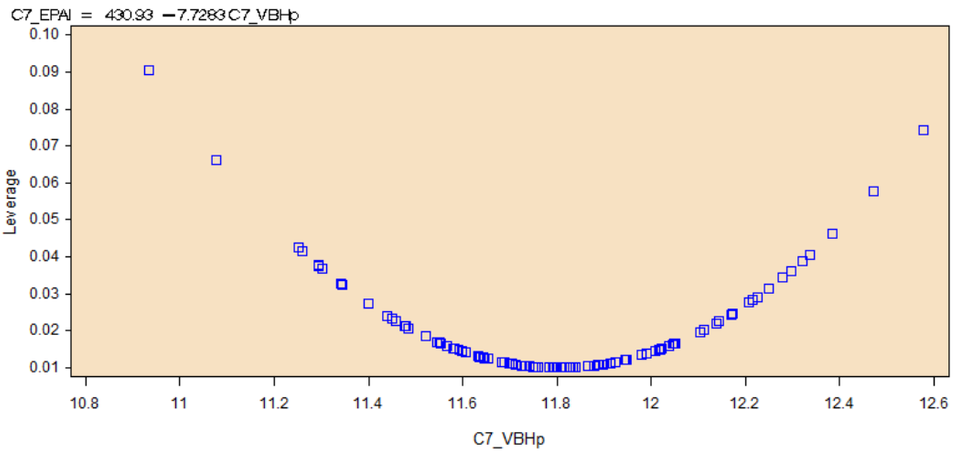

Fig. 8. Leverage vs. C7_VBHp

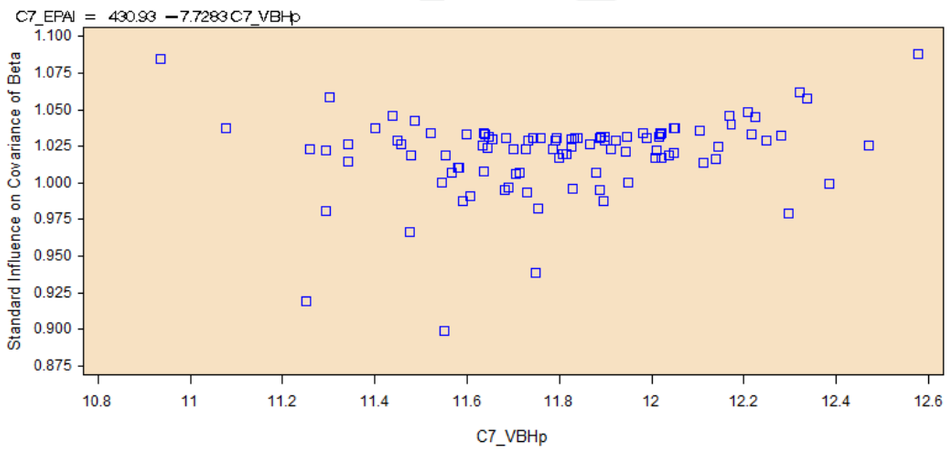

Fig. 9. Standard Influence on Covariance of Beta vs. C7_VBHp

- The lower endplate depth and the pedicle height on the right side (EPDl and PDHr)
- The upper endplate depth and the pedicle sagittal inclination on the left side (EPDu and PDIsl)
- The lower endplate transverse inclination and the spinal canal width (EPItl and SCW)
- The upper endplate transverse inclination and the posterior vertebral body height (EPItu and VBHp)
- The upper endplate transverse inclination and the pedicle area on the right side (EPItu and PDAr)
- The upper endplate width and the spinous process length (EPWu and SPL)
- The pedicle area on the left side and the pedicle sagittal inclination on the left side (PDAl and PDIsl)
- The pedicle height on the right side and the posterior vertebral body height (PDHr and VBHp)
- The pedicle height on the right side and the spinous process length (PDHr and SPL)
- The pedicle sagittal inclination on the left side and the anterior vertebral body height (PDIsl and VBHa)
- The pedicle sagittal inclination on the left side and the spinous process length (PDIsl and SPL)
- The pedicle transverse inclination on the right side and the spinal canal width (PDItr and SCW)

This type of relationship is important to note because it was thought that if there was a significance found in one comparison that the same type of relationship would be seen when doing the reciprocal comparison, but this was not always seen. When this type of relationship isn't seen it could be the result of the random number generation and the normal distribution of these numbers.

	ANOVA	Parameter Estimates		Y-intercept	Slope
	P	P (y-intercept)	P (regressor/ independent)		
EPDl vs. PDHr	0.0145	<0.0001	0.0145	19.19577	-0.59208
	Significant	Significant	Significant		
EPDl vs. EPAu	0.0227	<0.0001	0.0227	13.92929	0.00755
	Significant	Significant	Significant		
EPDu vs. EPAl	0.0499	<0.0001	0.0499	16.35341	-0.00366
	Significant	Significant	Not Significant		
EPDu vs. PDIsl	0.0149	<0.0001	0.0149	16.47022	0.04455
	Significant	Significant	Significant		
EPWu vs. SPL	0.0062	<0.0001	0.0062	20.24696	-0.02664
	Significant	Significant	Significant		
PDHr vs. EPDl	0.0145	<0.0001	0.0145	7.65744	-0.10034
	Significant	Significant	Significant		

Table 17. C7 Linear Measurements (Part 1)

	ANOVA	Parameter Estimates		Y-intercept	Slope
	P	P (y-intercept)	P (regressor/ independent)		
PDHr vs. VBHp	0.0153	<0.0001	0.0153	7.09761	-0.08508
	Significant	Significant	Significant		
PDHr vs. SPL	0.0454	<0.0001	0.0454	5.07412	0.01077
	Significant	Significant	Not Significant		
PDWr vs. PDIsr	0.0478	0.0002	0.0478	11.73842	-0.20069
	Significant	Significant	Not Significant		
SCW vs. EPItl	0.0143	<0.0001	0.0143	20.8603	-0.23411
	Significant	Significant	Significant		
SCW vs. PDItr	0.0218	<0.0001	0.0218	20.1399	-0.14708
	Significant	Significant	Significant		
SPL vs. EPWu	0.0062	<0.0001	0.0062	99.42223	-2.77358
	Significant	Significant	Significant		
SPL vs. PDHr	0.0454	<0.0001	0.0454	35.48384	1.84364
	Significant	Significant	Not Significant		
SPL vs. PDIsl	0.0208	<0.0001	0.0208	39.68142	-0.23022
	Significant	Significant	Significant		
VBHa vs. PDIsl	0.0274	<0.0001	0.0274	12.7251	0.04937
	Significant	Significant	Not Significant		
VBHp vs. PDHr	0.0153	<0.0001	0.0153	15.99891	-0.68864
	Significant	Significant	Significant		
VBHp vs. EPAl	0.0152	<0.0001	0.0152	14.38187	-0.00759
	Significant	Significant	Significant		
VBHp vs. EPItu	0.0064	<0.0001	0.0064	11.04194	0.10321
	Significant	Significant	Significant		

Table 18. C7 Linear Measurements (Part 2)

It is also of interest to see which correlations also existed in other vertebras, and if any existed throughout C3 to C7. There were eight correlations that were seen in more than just one vertebral segment. The link between the upper endplate width and the pedicle width on the right side (EPWu and PDWr) was seen in both the C4 vertebra and the C6 vertebra. As for the connection between the posterior vertebral body height and the pedicle area on the left side (VBHp and PDAl), this was seen in both the C4 vertebra and the C5 vertebra. The relationship between the spinous process length and the pedicle transverse inclination on the right side (SPL and PDItr) was seen in the C5 and C6

vertebra. The connection between the pedicle height on the right side and the lower endplate depth (PDHr and EPDl) was seen in both the C4 and C7 vertebra. The relationship between the upper endplate area and the lower endplate depth (EPAu and EPDl) was seen in both the C7 and C5 vertebra. The link between the lower endplate transverse inclination and the spinal canal width (EPItl and SCW) was seen in both C7 and C4. Also the connection between the upper endplate transverse inclination and the pedicle width on the right side (EPItu and PDWr) was seen in both the C5 and C7 vertebra. Finally the correlation between the pedicle transverse inclination on the right side and the spinous process length (PDItr and SPL) was seen in both the C5 and C6 vertebral segments. It would be of interest to investigate why this may be, and why there isn't a relationship present that was found in all 5 segments.

An example of some plots that resulted from the linear regression analysis of the vertebral segments through SAS® are shown in Figures 3-9. These figures are included to illustrate an example involving the lower endplate area and the posterior vertebral body height for the C7 vertebra (EPAl and VBHp).

In the study completed by Tan it was found that the endplate width and depth (EPW, EPD), and vertebral body height (VBH) are moderately constant from C3 to C5 and then increase to C7. The increase is more drastic in the endplate width than the end plate depth and vertebral body height, with the endplate depth and the vertebral body height having both a similar increasing trend. The posterior vertebral body height (VBHp), lower endplate width (EPWl), and the lower endplate depth (EPDl) are larger than their complementary measurements of anterior vertebral body height (VBHa), upper endplate width (EPWu) and the upper endplate depth (EPDu). As for the spinal canal, the width and depth (SCW and SCD) both are fairly constant from C3 to C6. The spinal canal width decreases sharply through to C7, and the spinal canal depth increases progressively into C7. Both the process lengths of the spinous and transverse (SPL and TPW) increase with a similar trend. The values of the left and right pedicle height (PDHl and PDHr) are comparatively similar, the same goes for the left and right pedicle width (PDWl and PDWr). The pedicle height (PDH) decreases gradually from C3 to C6 and then increases to C7. The pedicle width (PDW) increases throughout the cervical spine. The area of the lower and upper endplates (EPAl and EPAu) increases throughout the cervical spine, and the upper is at all times larger than the lower endplate area. The spinal canal area (SCA) increases from C3 to C5 and then decreases at C6 just to increase again to C7. Both the left and right pedicle area (PDAl and PDAr) are fairly constant from C3 to C5, but then the left increases to C7 while the right decreases to C7. The endplate inclinations for both the upper and lower regions (EPItu and EPitl) are angled toward the head with a steady inclination. The lower endplate transverse inclination is always smaller than the upper endplate transverse inclination. The pedicle sagittal inclination (PDIs) is fairly constant at about 40° from C3 to C6, but then at C6 the pedicles start to congregate towards each other. The pedicle transverse inclination (PDIt) is angled towards the back from C3 to C4 but then angle towards the head after C4 (Nissan and Gilad, 1984).

In comparing the endplate width and depth, the posterior vertebral body height, and the upper endplate area (EPW, EPD, VBHp, and EPAu) to Panjabi's study of the cervical spine of Caucasian subjects, Tan's measurements are smaller "by an average of 10.3%, 15.2%, 4.0%, and 8.3% respectively" than that of Panjabi's measurements. The lower endplate area (EPAl) are larger in Tan's study by 16.3% than Panjabi's. The trends of the vertebral body

measurements are similar in both Panjabi's and Tan's study. The mean difference for the spinal canal width (SCW) is about "-19.8% and -31.8% for the SCD." The trend of the spinal canal width, depth, and area (SCW, SCD, and SCA) were different in the two studies. The pedicle height and width (PDH and PDW) had a mean difference of -16.1% and -25.7% respectively when using the average of the left and right measurements. Spinal implants have been developed based on measurements from Caucasian specimens, and as can be seen the difference in the pedicle width shows that the design of these implants would not be a good fit for the population studied by Tan. For example a 5-mm transpedicle screw would not be able to fit because the pedicle width is not wide enough for it in the Chinese Singaporeans. The spinous process length (SPL) is smaller in Tan's study by about 5.5% and the transverse process width (TPW) is smaller by about 15.6% than Panjabi's study. But the spinous process length is slightly larger from C5 to C7 than Panjabi's study (Nissan and Gilad, 1984; Tan, Teo and Chua, 2004).

In the study completed by Panjabi it was found that their results generally agreed with previous studies completed by Liu, Nissan, and Francis. The front to back endplate dimensions were generally within 2 mm of measurements completed by Nissan and Francis, and also followed the same tendency from C2 to C7. The measurements from Liu were smaller than Panjabi's which could be a result of how measurements were found. The endplate area (EPA) also differed from Liu which is believed to be because Panjabi's area did not include the uncovertebral facet area while Liu's more than likely did. Panjabi's study saw that there was a widening in the spinal canal from C5 to C6 and then decrease at C7, while Francis' stated that the canal was relatively small throughout. The vertebral body height (VBH) were smaller by 2 to 2.5 mm than Nissan and Francis' study which is believed to be again because of the different measurement techniques (Francis, 1955; Liu, Clark and Krieger, 1986; Panjabi et al., 1991; Nissan and Gilad, 1984) .

	ANOVA	Parameter Estimates		Y-intercept	Slope
	P	P (y-intercept)	P (regressor/ independent)		
EPAl vs. EPDu	0.0499	<0.0001	0.0499	499.16617	-10.55392
	Significant	Significant	Not Significant		
EPAl vs. VBHp	0.0152	<0.0001	0.0152	430.9265	-7.72835
	Significant	Significant	Significant		
EPAu vs. EPDl	0.0227	0.0166	0.0227	112.68776	6.86404
	Significant	Significant	Significant		
PDAl vs. PDIsl	0.0197	<0.0001	0.0197	53.33933	0.63139
	Significant	Significant	Significant		
PDAr vs. EPItu	0.0162	<0.0001	0.0162	28.57023	0.46784
	Significant	Significant	Significant		

Table 19. C7 Area Measurements

	ANOVA	Parameter Estimates		Y-intercept	Slope
	P	P (y-intercept)	P (regressor/ independent)		
EPItl vs. SCW	0.0143	<0.0001	0.0143	10.06297	-0.25521
	Significant	Significant	Significant		
EPItl vs. EPAu	0.026	<0.0001	0.026	7.8214	-0.01266
	Significant	Significant	Not Significant		
EPItu vs. VBHp	0.0064	0.7368	0.0064	-1.01525	0.71055
	Significant	Not Significant	Significant		
EPItu vs. PDWr	0.0423	<0.0001	0.0423	6.34333	0.18166
	Significant	Significant	Not Significant		
EPItu vs. PDAr	0.0162	0.0357	0.0162	3.43319	0.12299
	Significant	Not Significant	Significant		
PDIsl vs. EPDu	0.0149	<0.0001	0.0149	-50.57442	1.32445
	Significant	Significant	Significant		
PDIsl vs. VBHa	0.0274	<0.0001	0.0274	-41.61664	0.98543
	Significant	Significant	Not Significant		
PDIsl vs. SPL	0.0208	<0.0001	0.0208	-19.73933	-0.2317
	Significant	Significant	Significant		
PDIsl vs. PDAl	0.0197	<0.0001	0.0197	-33.49084	0.08599
	Significant	Significant	Significant		
PDItr vs. SCW	0.0218	0.0011	0.0218	10.15645	-0.35731
	Significant	Significant	Significant		
PDItr vs. EPAu	0.042	0.7155	0.042	-0.67451	0.01729
	Significant	Not Significant	Not Significant		

Table 20. C7 Angular Measurements

1.5 Conclusion

The analysis of the cervical spines vertebral segments anthropometrics resulted in 600 total comparisons being completed in each vertebral body from C3-C7, resulting in 3000 comparisons in total being done. From this it was found that there were 11 relationships in the C3 vertebra, 23 in the C4 vertebra, 40 in the C5 vertebra, 22 in the C6 vertebra, and 34 in the C7 vertebra which is a total of 130 relationships found from C3 to C7. From this analysis it was found that only about $4\frac{1}{3}\%$ of the 3000 comparisons were significant. There were only 8 comparisons that were significant in more than one vertebral segment.

The relationships found between the dimensional anatomy of the vertebrae of the cervical spine will assist in accurate modeling of the spine as well as for device development helping to eliminate possible failure of devices due to improper fit within the region of the spine. This anthropometric data can also enable a better understanding of disease occurrence in certain alignments of the spine, and susceptibility of specific race, gender, or age groups. The results of this research will also allow for a better understanding of the functionality of the cervical spine and its susceptibility to failure.

2.1 Cervical spine finite element modeling methods review

The cervical spine is one of the most important physiologic systems in the human body. The cervical spine offers primary stability to the head neck system along with protecting the spinal cord. The cervical spine features higher levels of motion and flexibility as compared to the other spine regions. The spines flexibility and motion does leave it susceptible to a higher rate of injury as compared to the other spine regions (Ng and Teo, 2001). It is therefore important to study the spine to gain a better understanding of the behavior spine. In-vivo studies of the cervical spine can provide information on the behavior of the spine under specific conditions. However, an in-vivo analysis of the spine cannot provide specific load response information at the vertebral and intervertebral disc level. In contrast, in-vitro analysis of the cervical spine can provide load displacement response at vertebral segments. In-vitro analyses of the cervical spine are limited to load displacement results; they cannot provide internal response characteristics such as stress and strain (Yoganandan et al., 1996; Panagiotopoulou, 2009). As such, there has been growing interest and application of finite element (FE) methods in the study of the cervical spine. Finite element models of the cervical spine have been used to study spine biomechanics, injuries, and response to medical interventions (Yoganandan, Kumaresan and Pintar, 2001; Pitzen et al., 2002; Pitzen, Matthis and Steudel, 2002)

Development of a finite element model of the spine involves several key areas of consideration. A finite element model of the spine must aim to accurately represent the anatomical features of the spine. Spinal vertebrae, intervertebral discs, ligaments, and their interrelation must all be carefully considered in the development of a model (Kallemeyn, Tadepalli and Shivanna, 2009; Bogduck and Yoganandan, 2001). The methods applied in constructing the finite element model play an important role in its ability to accurately represent the cervical spine. The finite element methods applied in analyzing a cervical spine model play are also of extreme import (Yoganandan, Kumaresan and Pintar, 2001; Yoganandan et al., 1996). In order to gain a better understanding of cervical spine finite element modeling and analysis, a review of the pertinent literature was performed.

2.2 Cervical Spine Analysis

Mathematical modeling approaches allow for both static and dynamic analysis of the cervical spine. Dynamic analyses of the spine often aim to characterize the response of the cervical region during an impact with the goal of better understanding vehicular injury scenarios such as whiplash. Dynamic models of the cervical spine often include the entire cervical spine, and the head. Vertebral bodies have been modeled as rigid bodies, with soft tissues such as spinal ligaments represented by linear springs (Esat, 2005; Brolin and Halldin, 2005; Brolin and Halldin, 2004; Stemper et al., 2006). This modeling approach somewhat limits the load response data that can be derived for specific vertebral bodies and intervertebral discs.

Static FE analyses focus on analysis of load response characteristics of cervical spine segments. In an effort to represent the load response as accurately as possible, static FE models are constructed with as much detail as possible. (Kallemeyn, Tadepalli and Shivanna, 2009; Panzer and Cronin, 2009; Goel and Clausen, 1998; Ha, 2006). In contrast to dynamic models, static models often focus on two to three vertebral bodies as opposed to the complete cervical spine. These functional spinal units (FSU) can provide important internal load and segment displacement data (Ng et al., 2003). Static analyses also allow for corroboration of FE results with in vitro study load displacement results. Static analyses have been used to analyze a variety of topics including spinal column biomechanics, soft tissue effects on behavior, soft and hard tissue injuries, and even prosthetic disc replacements (Zhang et al., 2006; Voo et al., 1997; Noailly et al., 2007; Ha, 2006; Galbusera et al., 2008).

As stated, static element analyses lend themselves well to validation of cervical spine finite element models. Validation of any finite element model is an extremely important process the confirms that the model and assumptions there in, adequately represent that actual physical spine. There have been in-vitro studies of the cervical spine and spine segments that can act as comparison and validation cases for finite element studies (Moroney et al., 1988; Panjabi et al., 2001; Richter et al., 2000). In order to use an in-vitro study as a comparison case, test conditions including loading and constraints must be equivalent. This does not however limit the loading cases applied to finite element studies to those already employed in-vitro. By verifying a study under known in-vitro conditions investigators can assume the response of the finite element model is valid for a certain range then continue to test different scenarios (Ng et al., 2003). The following summary table, Table 21, provides study types, load conditions and validation methods employed.

Author	**Year**	**Study Type**	**Spine Levels**	**Loading**	**BC**	**Validation**
Li et al. (Li and Lewis, 2010)	2010	Static Surgery	All Segment	0.33 - 2 Nm Flexion Extension Lateral Bending Axial Rotation 1 Nm + 73.6 Compression	Inferior Endplate Fully Fixed	Panjabi et al. 2001 Wheeldon et al. 2006
Kallemeyn et al. (Kallemeyn, Tadepalli and Shivanna, 2009)	2009	Static Biomechanics	2 Segment	1 Nm Flexion Extension Lateral Bending Axial Rotation + 73.6 N Compression 600 N Compression	Inferior Endplate Fully Fixed	(Moroney et al., 1988; Traynelis et al., 1993; Pintar et al., 1995)
Panzer et al. (Panzer and Cronin, 2009)		Static Biomechanics	2 Segment	0.3 – 3.5 Nm Flexion Extension Lateral Bending Axial Rotation	Inferior Endplate Fully Fixed	Goel et al. 1988 Voo et al. 1997 Maurel et al. 1997 Moroney et al. 1998

Author	Year	Study Type	Spine Levels	Loading	BC	Validation
Galbuseara et al. (Galbusera et al., 2008)	2008	Static Prosthesis	4 Segment	2.5 Nm Flexion Extension + 100 N Compression	Inferior Endplate Fully Fixed	In-vitro (Wheeldon et al., 2006)
Greaves et al. (Greaves, Gadala and Oxland, 2008)		Static Injury	3 Segment	Injury based deflection	Injury based	In-vivo Hung et al. 1979 Maiman et al. 1989
Wheeldon et al. (Wheeldon et al., 2008)		Static Biomechanics	4 Segment	0 – 2 Nm Flexion Extension Axial Rotation	Inferior Endplate Fully Fixed	Gilad & Nissan 1986 Panjabi et al. 1991
Teo et al. (Teo et al., 2007)		Static Mesh Generation	7 Segment	N/A	Inferior Endplate Fully Fixed	N/A
Ha (Ha, 2006)	2006	Static Prosthesis	4 Segment	1 Nm Flexion Extension Lateral Bending Axial Rotation	Inferior Endplate Fully Fixed	Moroney et al. 1991 Pelker et al. 1987 Goel et al. 1998 Teo & Ng et al. 2001
Zhang et al. (Zhang et al., 2006)		Static Biomechanics	8 Segment	1 Nm Flexion Extension Lateral Bending Axial Rotation 50 N Compression	Inferior Endplate Fully Fixed	Goel et al. 1984 Moroney et al. 1988 Goel & Clausen 1998 Panjabi et al. 2001
Haghpanahi & Mapar (Haghpanahi, 2006)		Static Biomechanics	5 Segment	1.8 Nm Flexion Extension	Inferior Endplate Fully Fixed	Lopez-Espinea (FEA) 2004 Goel et al. Voo et al. Maurel et al. Moroney et al.
Esat et al. (Esat, 2005)	2005	Dynamic Biomechanics	3 Segment	1.6 Nm Flexion Extension 73.6 N Compression	Inferior Endplate Fully Fixed	Shea et al. 1991
Brolin et al. (Brolin and Halldin, 2004)	2004	Static Biomechanics	2 Segment	1.5, 10 Nm Flexion Extension Lateral Bending Axial Rotation 1500 N Tension	Inferior Endplate Fully Fixed	Panjabi et al. 1991 Panjabi et al. 1991 Van et al. 2000 Goel et al. 1990

Author	Year	Study Type	Spine Levels	Loading	BC	Validation
Ng et al. (Ng et al., 2003)	2003	Static Injury	3 Segment	1.8 Nm Flexion Extension Lateral Bending Axial Rotation 73.6 N Compression	Inferior Endplate Fully Fixed	Shea et al. 1991 Moroney et al. 1988 Pelker et al. 1991 Maurel et al. 1997 Goel et al. 1998
Bozkus et al. (Bozkus et al., 2001)	2001	Static Injury	1 Segment	200 – 1200 N Compression	Inferior Endplate Fully Fixed	Cadaver Study
Teo et al. (Teo and Ng, 2001)		Static Biomechanics	3 Segment	1 mm Axial Displacement	Inferior Endplate Fully Fixed	Shea et al. 1991 Yoganandan et al. 1996 (FEA)
Graham et al. (Graham et al., 2000)	2000	Static Injury	1 Segment	1279, 1736 N Compression	Inferior Endplate Fully Fixed	Doherty et al 1993
Kumaresan et al. (Kumaresan et al., 2000)		Static Biomechanics	3 Segment	0.5 Nm Flexion Extension 200 N Compression	Inferior Endplate Fully Fixed	FEA Kumaresan et al. 1997
Zheng et al. (Zheng, Young-Hing and Watson, 2000)		Static Surgery	5 Segment	196 N Compression	Injury Case Dependent	
Kumaresan et al. (Kumaresan et al., 1999)	1999	Static Biomechanics	3 Segment	0.5 – 1.8 Nm Flexion Extension Lateral Bending Axial Rotation	Inferior Endplate Fully Fixed	Cadaver Study Pintar et al. 1995
Kumaresan et al. (Kumaresan, Yoganandan and Pintar, 1999)		Static Biomechanics	3 Segment	1.8 Nm Flexion Extension Lateral Bending Axial Rotation 125 – 800 N Compression	Inferior Endplate Fully Fixed	Moroney et al. 1988
Goel et al. (Goel and Clausen, 1998)	1998	Static Biomechanics	2 Segment	1.8 Nm Flexion Extension Lateral Bending Axial Rotation 73.5 N Compression	Inferior Endplate Fully Fixed	Moroney et al. 1988 Clausen et al. 1996 Goel et al. 1988 Teo et al. (FEA) 1994

Author	Year	Study Type	Spine Levels	Loading	BC	Validation
Kumaresan et al. (Kumaresan et al., 1998)		Static Biomechanics	2 Segment	Flexion Extension Lateral Bending Compression	Inferior Endplate Fully Fixed	N/A
Maurel et al. (Maurel, Lavaste and Skalli, 1997)	1997	Static Biomechanics	5 Segment	0 – 1.6 Nm Flexion Extension Lateral Bending Axial Rotation 6 N Compression	Inferior Endplate Fully Fixed	Cressend 1992 Panjabi et al. 1986 Wen 1993 Wen et al. 1993 Moroney et al. 1984, 1998
Voo et al. (Voo et al., 1997)		Static Surgery	3 Segment	1.8 Nm Flexion Extension Lateral Bending Axial Rotation	Inferior Endplate Fully Fixed	Liu et al. 1982 Moroney et al. 1988
Yoganandan et al. (Yoganandan et al., 1996)	1996	Static Biomechanics	3 Segment	1 mm Compression	Inferior Endplate Fully Fixed	Shea et al. 1991
Bozic et al. 1994 (Bozic et al., 1994)	1994	Static Injury	1 Segment	3400 N Compression	Inferior Endplate Fixed by Spring	

Table 21. Cervical Spine Finite Element Modeling Summary Table

The study by Esat et al. (Esat, 2005) combines both static and dynamic analysis methods. The investigators aimed to simulate the response of the head and neck system under frontal and rear impact scenarios. A multi-body dynamic head and neck computational model was developed and validated using human volunteer experimental data. The investigators take the analysis further by developing a finite element model of the cervical spine and intervertebral discs. The finite element model was used to study the response of the intervertebral discs to the dynamic load cases (Esat, 2005). The study illustrates the flexibility of employing the finite element method in the analysis of the cervical spine. A study by Sung Kyu Ha employed a finite element model of the cervical spine to study the effects of spinal fusion and the implantation of a prosthetic disc on spine behavior (Ha, 2006). Spinal fusion was modeled by applying a graft with material properties of the cortical bone between adjacent vertebral segments. The disc prosthesis was modeled by replacing the entire intervertebral disc with an elastomer core. Efforts were made to select an elastomer core with similar properties to that of the intervertebral disc. The analysis results showed that spinal fusion led to a 50 – 70% reduction in range of motion for the fused spinal segment. The introduction of a prosthetic disc did not change the range of motion seen in the motion segment (Ha, 2006). Using a validated finite element model of the cervical spine, the study was able to help predict the effect of two interventions that are often employed in spinal injury cases.

2.3 Hard tissue modeling

As stated, the accuracy of an FE model at representing the cervical spine anatomy is of extreme importance. There are two prominent modeling methods in the development of cervical spine vertebral body models. Multi axis digitizers can be used to map points along the vertebral bodies. The data set of points can then be used to create a model via a computer aided drafting package. This approach can be applied to the development of two dimensional (2D) and three dimensional (3D) models (Zhang et al., 2006; Esat, 2005; Haghpanahi, 2006; Panzer and Cronin, 2009). Haghpanahi et al. used the data point approach to create a parameterized 2D model of the C3 – C7 vertebral model. Intervertebral discs were modeled in relation to adjacent vertebral pairs (Haghpanahi, 2006).

Digitizing the surface geometry of cervical spine segments is somewhat limited by the number of points plotted. A look at the vertebral segment by Haghpanahi shows that surfaces are somewhat linear. The vertebral endplates and posterior elements are represented by straight line segments which do not convey the actual curvature and undulations of the vertebra. An alternative hard tissue modeling approach is to use computed tomography (CT) scan data. The process involves digitizing CT scans and using the data to create a vertebral model. In a study by Yoganandan et al., investigators used NIH-Image and an edge detection algorithm they developed to process the CT scans of the spine. The data extracted from NIH-Image provided edge locations for the vertebral bodies which were used to create wire frames of each vertebral body (Yoganandan et al., 1997). A decade later, a study by Sung Kyu Ha used the Amira image processing software to digitize CT scans, with 3D models and meshes generated in RapidForm and Ansys respectively (Ha, 2006). Though the two methods both yielded anatomically correct vertebral models, the process employed by Ha involved much less manual tasks and offered a higher level of refinement.

Regardless of the methods employed to develop the 3D model of the vertebral bodies, for the purposes of finite element analysis, a finite element mesh of the part must be developed. Element selection is of paramount importance in developing any finite element mesh. Element selection is dependent on several factors including, the type of analysis to be performed, and the geometry of the body to be meshed to name a few. Cervical spine vertebral bodies can be adequately meshed with 4 noded solid tetrahedral elements; however 8 noded hexahedral elements are preferred (Bozkus, 2001; Teo et al., 2007). Vertebral bodies are made up of two bone regions, the cancellous core and cortical shell. The cortical shell can be modeled as separate region of distinct thickness. The region can be modeled with a separate set of solid or shell elements (Yoganandan, Kumaresan and Pintar, 2001). The final hard tissue areas that must be considered during modeling are the vertebral body facet joints. The facet joints play an important role in stabilizing and constraining the motion of adjacent vertebral bodies. There are a myriad of modeling methods employed in approximating facet joints and their behavior. A summary of mesh methods employed in vertebral body modeling is provided in Table 22.

Author	Year	Source	Cancellous	Cortical	Facet Joints
Yuan et al. (Li and Lewis, 2010)	2010	CT	4 node tetrahedral	3 node shell element	

Author	Year	Source	Cancellous	Cortical	Facet Joints
Kallemeyn et al. (Kallemeyn, Tadepalli and Shivanna, 2009)	2009	CT	8 node hexahedral	8 node hexahedral	Pressure over closure relationship
Panzer et al. (Panzer and Cronin, 2009)		CAD	3D hexahedral	2D quadrilateral	Squeeze film bearing relationship
Galbuseara et al. (Galbusera et al., 2008)	2008	CT	8 node hexahedral	8 node hexahedral	Frictionless surface-based contact
Greaves et al. (Greaves, Gadala and Oxland, 2008)		CT	8 node brick	8 node brick	
Wheeldon et al. (Wheeldon et al., 2008)		CT	Solid	Solid	Solid / fluid hydraulic incompressibl e
Teo et al. (Teo et al., 2007)		CT	Hexahedral Tetrahedral	Hexahedral Tetrahedral	
Ha (Ha, 2006)	2006	CT	20 node brick	8 node shell	Non-linear contact element
Zhang et al. (Zhang et al., 2006)		CAD	8 node brick	8 node brick	Surface to surface contact
Haghpanahi & Mapar (Haghpanahi, 2006)		CAD	solid	solid	
Esat et al. (Esat, 2005)		CAD	8 node brick	8 node brick	
Brolin et al. (Brolin and Halldin, 2004)	2004	CT	8 node brick	4 node shell	Sliding contact with friction
Ng et al. (Ng et al., 2003)	2003	CAD	8 node solid	8 node solid	Nonlinear contact
Bozkus et al. (Bozkus et al., 2001)	2001	CT	Solid / 4 node tetrahedral		
Teo et al. (Teo and Ng, 2001)		CAD		8 node solid	
Graham et al. (Graham et al., 2000)	2000	CT	tetrahedral	Tetrahedral thin shell	
Kumaresan et al. (Kumaresan et al., 2000)		CT	8 node brick	8 node brick	8 node, fluid, membrane elements
Zheng et al. (Zheng, Young-Hing and Watson, 2000)		CT	10 node tetrahedral	10 node tetrahedral	
Kumaresan et al. (Kumaresan et al., 1999)	1999	CT	8 node brick	8 node brick	8 node, fluid, membrane elements

Author	Year	Source	Cancellous	Cortical	Facet Joints
Kumaresan et al. (Kumaresan, Yoganandan and Pintar, 1999)		CT	8 node brick	8 node brick	8 node, fluid, membrane elements
Goel et al. (Goel and Clausen, 1998)	1998	CT	8 node brick	8 node brick	
Kumaresan et al. (Kumaresan et al., 1998)		CT	8 node brick	8 node brick	8 node, fluid, membrane elements
Maurel et al. (Maurel, Lavaste and Skalli, 1997)	1997	CT	8 node	8 node	Gap element
Voo et al. (Voo et al., 1997)		CT	8 node solid	thin shell	
Yoganandan et al.	1996	CT	8 node solid	thins shell	
Bozic et al. 1994 (Bozic et al., 1994)	1994	CT	8 node solid	8 node solid	

Table 22. Cervical Spine Vertebral Modeling Methods

2.4 Intervertebral disc modeling

Intervertebral discs (IVD) are extremely important to the behavior of the spine. Intervertebral discs act as dampers responding to compressive forces within the spine (Yoganandan, Kumaresan and Pintar, 2001). Discs are made up of two distinct regions, the outer annulus fibrosus ring, and an inner nucleus pulposus core (Ha, 2006). Both regions are largely fluid based. The annulus fibrosus is made up of collagen fibers embedded in an extracellular matrix composed of water and elastin fibers. Collagen fibers are arranged as a structure of rings throughout the annulus region. Fibers are oriented between 25° and 45° with respect to the horizontal plane. Collagen fibers provide primary stiffness to the annulus region (Ambard and Cherblanc, 2009; Noailly, Lacoix and Planell, 2005). Discs interact with adjacent vertebral bodies via the cartilaginous endplates.

Considerations must be made to accurately model IVD behavior. Modeling IVD must be approached in a different manner than the vertebral bodies as CT scans do not provide soft tissue data. Cryomicrotomy images can be used as an alternative to fill in the missing soft tissue data (Yoganandan, Kumaresan and Pintar, 2001; Voo et al., 1997). An alternative to employing cryomicrotomy is to model intervertebral discs in reference to their interaction with related solid bodies (Yoganandan, Kumaresan and Pintar, 2001). An advantage of IVD modeling is their relative simple geometry in comparison with vertebral bodies. An IVD can be modeled with a CAD package as a cylindrical disc (Meakin and Huskins, 2001). For finite element analysis purposes the intervertebral disc annulus is often modeled as a fiber reinforced composite. Solid brick elements will be reinforced by a fiber or rebar element matrix of alternating angular orientation. The reinforcing fibers often employ a nonlinear response behavior unique to that of the solid annuls elements they are suspended within. The nucleus has been modeled as an incompressible fluid (Eberlein, Holzapfel and Froelich, 2004). This approach can involve modeling the nucleus with specific incompressible fluid elements. Though ideal, this approach presents a level of complexity that cannot be attained in all studies. The alternative involves applying general modulus and poison's ratio to the nucleus region (Ha, 2006) Table 23. summarizes finite element modeling approaches employed for the IVD.

Author	Year	Disc Components	Elements
Li et al. (Li and Lewis, 2010)	2010	Annulus fibrosus Nucleus pulposus	8 node brick 4 node tetrahedral
Kallemeyn et al. (Kallemeyn, Tadepalli and Shivanna, 2009)	2009	Annulus fibrosus Nucleus pulposus	8 node tetrahedral Hydrostatic fluid
Panzer et al. (Panzer and Cronin, 2009)		Annulus fibrosus Nucleus pulposus	Hexahedral element Incompressible element
Galbuseara et al. (Galbusera et al., 2008)	2008	Annulus fibrosus Nucleus pulposus	Hexahedral element Tension only truss
Wheeldon et al. (Wheeldon et al., 2008)		Annulus fibrosus Nucleus pulposus	Solid element Rebar element Incompressible fluid
Palomar et al. (Palomar, Calvo and Doblare, 2008)		Annulus fibrosus Nucleus pulposus	Solid element Linear tetrahedral Incompressible fluid
Schmidt et al. (Schmidt, 2007)	2007	Annulus fibrosus Nucleus pulposus	8 node solid element 3D spring element Incompressible Hyper elastic
Ha (Ha, 2006)	2006	Annulus fibrosus Nucleus pulposus	20 node solid element Tension only spar
Zhang et al. (Zhang et al., 2006)		Annulus fibrosus Nucleus pulposus	8 node brick
Eberlin et al. (Eberlein, Holzapfel and Froelich, 2004)	2004	Annulus fibrosus Nucleus pulposus	8 & 20 node hexahedral Incompressible fluid
Meakin et al. (Meakin and Huskins, 2001)	2001	Annulus fibrosus Nucleus pulposus	Solid element Fluid element
Kumaresan et al. (Kumaresan et al., 2000)	2000	Annulus fibrosus Nucleus pulposus	8 node solid Tension only rebar 3D fluid element
Kumaresan et al. (Kumaresan et al., 1999)	1999	Annulus fibrosus Nucleus pulposus	8nnode solid Rebar element ncompressible fluid
Maurel et al. (Maurel, Lavaste and Skalli, 1997)	1997	Annulus fibrosus Nucleus pulposus	8 node element Cable element
Voo et al. (Voo et al., 1997)		Uniform disc	8 node element
Yoganandan et al. (Yoganandan et al., 1996)	1996	Uniform disc	8 node element
Bozic et al. 1994 (Bozic et al., 1994)	1994	Uniform disc	Springs element

Table 23. Cervical Spine Intervertebral Disc Modeling Methods

The IVD disc modeling summary table illustrates an acceptance of modeling the two distinct regions, the nucleus pulposus and intervertebral disc. As stated, the approaches employed do vary. In modeling the annulus fibrosus, the inclusion or exclusion of the fiber reinforcing matrix is a key modeling point. A study by Palomar (Palomar, Calvo and Doblare, 2008) illustrates the level of detail that can be employed in modeling the annulus fibrosus fiber matrix. The authors used in-vitro data sourced from a specific analysis of the tensile behavior of multiple layers of annulus under very slow strain (Ebara et al., 1996). The data

was used to adjust material properties of a strain energy function developed for annulus fibers (Holzapfel, 2000). The mathematical model was then implemented via a UMAT user subroutine in the Abaqus finite element software package (Palomar, Calvo and Doblare, 2008). It is clear that this approach focused on developing a realistic intervertebral disc model. The model allowed for greater understanding of internal stress response of the intervertebral discs.

2.6 Cervical spine ligament modeling

Ligaments are the supportive connective structures of the spine. Ligaments of the spine include the ligamentum flavum (LF), interspinous ligament (ISL), capsular ligament (CL) and intertransverse (ITL) ligaments. This set of ligaments function to support individual vertebra. The anterior longitudinal (ALL), posterior longitudinal (PLL), and the supraspinous ligament (SSL) act as supports for series of vertebra (Yoganandan, Kumaresan and Pintar, 2001). Spinal ligaments are often modeled based on knowledge of their anatomical makeup, locations, and relation to vertebra and intervertebral discs as they are not represented in CT images. There is data available providing ligament cross sectional area, length, and mechanical behavior. For finite element purposes, ligaments are most often represented as non linear tension only entities. Spring, cable, truss, and tension only elements have all been employed in the modeling of ligaments (Yoganandan, Kumaresan and Pintar, 2001). A summary of some ligament modeling techniques applied is provided in Table 24.

Author	Year	Ligaments	Behavior	Elements
Li et al. (Li and Lewis, 2010)	2010	ALL, PLL, CL, LF, ISL, TL, APL	Nonlinear	Tension-only spar
Kallemeyn et al. (Kallemeyn, Tadepalli and Shivanna, 2009)	2009	ALL, PLL, CL, LF, ISL	Nonlinear	2 node truss
Panzer et al. (Panzer and Cronin, 2009)		ALL, PLL, CL, LF, ISL	Nonlinear	1D tension only
Galbuseara et al. (Galbusera et al., 2008)	2008	ALL, PLL, CL, LF, ISL	Nonlinear	Spring element
Greaves et al. (Greaves, Gadala and Oxland, 2008)		ALL, PLL, CL, LF, ISL	Nonlinear	2 node link
Palomar et al. (Palomar, Calvo and Doblare, 2008)		ALL, PLL, YL, ISL, ITL	Nonlinear	Tension only truss
Wheeldon et al. (Wheeldon et al., 2008)		ALL, PLL, LF, CL, ISL	Nonlinear	Spring element
Schmidt et al. (Schmidt, 2007)	2007	ALL, PLL, CL, LF, ISL, SSL	Force deflection curve	Spring element
Ha (Ha, 2006)	2006	ALL, PLL, LF, ISL, CL	Nonlinear	Tension only spar
Zhang et al. (Zhang et al., 2006)		ALL, PLL, SSL, ISl, LF, CL, AL, TL, NL, APL	Linear	2 node link
Brolin et al. (Brolin and Halldin, 2004)	2004	ALL, PLL, TL, LF, CL, ISL	Force deflection curve	Tension only spring
Eberlin et al. (Eberlein, Holzapfel and Froelich, 2004)		ALL, PLL, TL, LF, CL, ISL	Nonlinear	Membrane element

Author	Year	Ligaments	Behavior	Elements
Kumaresan et al. (Kumaresan et al., 2000)	2000	ALL, PLL, CL, LF, ISL	Nonlinear	Tension only element
Kumaresan et al. (Kumaresan, Yoganandan and Pintar, 1999)	1999	ALL, PLL, CL, LF, ISL	Nonlinear	Tension only element
Maurel et al. (Maurel, Lavaste and Skalli, 1997)	1997	ALL, PLL, CL, Lf, ISl, SSL	Nonlinear	Tension only cable element
Voo et al. (Voo et al., 1997)		ALL, PLL, CL, LF, ISL	Linear	2 node uniaxial
Yoganandan et al. 1996 (Yoganandan et al., 1996)	1996	N/A	N/A	N/A
Bozic et al. (Bozic et al., 1994)	1994	N/A	N/A	N/A

Table 24. Cervical Spine Ligament Modeling Methods

The summary table clearly illustrates that despite the difficulties of visualizing spinal ligaments for modeling purposes; they are still included in most cervical spine finite element models. It is also evident that the majority of investigators aim to capture the nonlinear behavior of cervical spine ligaments. The degree to which ligament nonlinearity has been captured does vary amongst studies. The use of finite elements with nonlinear characteristics has been applied and deemed adequate (Ha, 2006). Non linearity can be further implemented by employing strain dependent modulus of elasticity values to the finite element model ligaments. Strain dependent moduli of elasticity are often sourced from in vitro experimentation of cervical spine segments (Kallemeyn, Tadepalli and Shivanna, 2009; Yoganandan, Kumaresan and Pintar, 2000). Strain dependent moduli of elasticity invariably add complexity to any mathematical analysis procedure. Additionally strain limits are vary greatly depending on the in-vitro data sourced and are subject to variability and questions of applicability to the current study. Despite the shortfalls it is clear from a review of the literature that investigators are continually developing and applying sophisticated modeling techniques to spinal ligaments.

2.7 Discussion

The review of cervical spine modeling techniques has illustrated the FEA can be a powerful tool in the study of cervical spine behavior, injury, and treatment. There have been studies the focus on finite element models of the as tools in the design of spine prostheses (Galbusera et al., 2008; Ha, 2006; Meakin and Huskins, 2001). Ha et al. developed a multi segment model of the cervical spine and continued to analyze its behavior with and without an elastomer-type prosthetic disc. The study aimed to design the prosthetic disc that would most closely reflect the behavior of the spinal unit with a disc present. The study found that a disc with a modulus of 5.9 MPa would maintain biomechanical behavior of the complete spine. The authors even note that the modulus value found could be achievable using polyurethane. Determining a modulus value numerically provides a good basis for which to start designing an IVD prosthesis that maintains biomechanical function (Ha, 2006).

Finite element analysis models have even begun to be applied to juvenile spinal models including juvenile anatomical features such as joint plates (Wheeldon et al., 2008; Sairyo et al., 2006; Sairyo et al., 2006). Models have also continued to better represent the spine not only in geometry but in behavior. Studies have been undertaken to develop accurate material and behavioral models based on extensive concurrent in-vitro testing (Yoganandan, Kumaresan and Pintar, 2001; Eberlein, Holzapfel and Froelich, 2004).

In studying fracture in the atlas Teo et al. developed a single entity model of the atlas. Material property data from the literature were employed and a series of load to failure FE analyses were performed. The study predicted stress distributions along the atlas and maximal loads. Though this data cannot be directly applied in a clinical sense, it can be qualitatively applied to future in-vitro or mathematical modeling (Teo and Ng, 2001). Models have progressed from going without ligaments (Yoganandan et al., 1996; Bozic et al., 1994), to focusing specifically on calibrating ligament material properties (Brolin and Halldin, 2004). Similar advances can be seen in IVD disc modeling which has gone from a simple spacer of uniform material properties (Bozic et al., 1994) to highly advanced nonlinear constitutive models of IVD behavior (Palomar, Calvo and Doblare, 2008). The variation in study types and analysis methods underscore the effectiveness, and flexibility of applying FE methods to the study of the cervical spine.

3.1 Finite element analysis of superior C3 cervical vertebra endplate and cancellous core under static loads

Subsidence is a failure mechanism that can occur after implantation of an intra vertebral implant device. Subsidence is clinically defined as the loss of postoperative intervertebral disc height and has been shown to occur in as many as 77% of patients after fusion surgeries (Choi and Sung, 2006). According to actuarial rates subsidence occurs at 63.4 and 70.7 percent at 12 and 16 weeks respectively (Choi and Sung, 2006). Occurrences of subsidence could be due to bone failure, which may be attributed to compressive stresses, or a failure of the implanted device specifically bone graft material (Jost et al., 1998). While a loss of height is common, measuring it may be contentious. Identifying the edge of the device proves difficult due to bone in-growth and the shadow of the apophyseal ring. Significant subsidence has been defined differently for the lumbar and cervical regions of the spine. Losses of disc height of 2mm in the lumbar spine and 3mm in the cervical spine have been considered relevant benchmarks (Choi and Sung, 2006; Van Jonbergen et al., 2005; Kulkarni et al., 2006). Another indication of subsidence is the change in lordic curve of the cervical spine. Changes in angle between the endplates, at the surgical level in the case of fusion, would indicate that the device is sinking into the vertebral bodies. Angle changes have been measured at a lordic increase of 1.6 degrees postoperatively to a follow up lordic decrease of 2.5 degrees (Kulkarni et al., 2006). The reduction in angle indicates that either the anterior or posterior part of the implanted device had subsided into the vertebral body. This failure is also a localized failure that is initiated by high contact forces generated by implanted disc devices.

Understanding the endplate morphology and biomechanics is crucial to the future success rates of implanted devices. The previous section of this chapter talked extensively about the type of data collected and measured. Several studies have been aimed at determining the thickness, strength and density of the vertebral endplates of the cervical spine by directly measuring cadaver specimens. The thickest regions are in the posterior region of the superior endplate and the anterior region of the inferior endplate with the central region being the thinnest area (Panjabi et al., 2001; Pitzen, 2004; Edwards et al., 2001). Mechanically the thicker regions of the endplate are stronger than the thinner areas (Grant et al, 2001; Oxland, 2003). Oxland showed that the thinner, middle lumbar region had a mean failure load between approximately 60-100 N, and increased toward the endplate's periphery, thicker regions, to a load of approximately 175 N (Grant et al, 2001). Locations of thicker endplate bone are indicative of other factors that affect the biomechanical quality of the

endplate. Density scans of the endplate, as measured by peripheral quantitative computed tomography (pQCT) scans, reveal that the endplate bone is denser in thicker regions (Ordway et al., 2007). Results show that an increase in bone density from 150 to 375 mg/mm^3 equates to an approximate stiffness increase from 100 to 200 N/mm. These same regions, which have a greater density and are thicker, also have an increased mineral deposition than thinner regions of the cervical endplates (Muller-Gerbl et al., 2008; Panzer et al., 2009). The increased mineral deposits were located in areas of the endplate that typically have the highest indentation test results and therefore higher failure limits (Grant et al, 2001; Oxland, 2003; Muller-Gerbl et al., 2008; Panzer et al., 2009).

Causes of subsidence can be modeled using finite element models. As previously discussed finite element modeling allows the investigation of several parameters like stress strain and deformations of irregularly shaped objects. The complex anatomical features previously discussed can be modeled with finite element methods to create a theoretical model that can be validated using experimental methods. This should increase the reproducibility of the model in many different scenarios to analyze different aspects of the cervical spine, in this case specifically the vertebral bodies. Frequently theoretical vertebral geometry is constructed from anthropometric data (Polikeit et al., 2003; Denoziere and Ku, 2006). The anthropometric data is typically compiled from measurements taken on a large sample group of cadavers. Theoretical models usually assume geometric properties of parameters that are difficult to measure directly and cost effectively, for example cortical shell thickness. Experimental models built from CT's also have material property limitations but are well suited for replicating anthropometric geometry for a single user. In both cases some assumptions need to be made concerning shell thicknesses. Several studies simplify the cortical shell and endplates as a shell with constant or only a slight variation in the endplate. The goal of the following study is to determine if an endplate thickness of a half-millimeter is an adequate approximation for the vertebral endplate by comparing endplate stresses.

3.2 Methods

A 3-dimensional linear elastic model of the C3 vertebrae was constructed from CT images of a 25-year old female that consisted of the vertebrae's bony structure. MIMICS 13.0 (Materialise, Ann Arbor, Michigan, USA) was used to convert the CT images to a 3-D model. The 3D model was smoothed and meshed using 3-Matic (Materialise, Ann Arbor, Michigan, USA). From 3-Matic an orphan mesh was imported into Abaqus 6.9 (Simulia, Providence, Rhode Island, USA) finite element design suite for post-processing. This experiment considers the thickness of the superior vertebral endplate. The superior endplate was modeled in four different ways, labeled Model 1 through Model 4. The first model, Model 1, used half-millimeter thick shell elements as an approximation for the superior endplate. Model 2 assumes the endplate has been completely removed. The removal was modeled by the actual removal of the shell elements exposing the volume elements of the core. Model 3 had a superior endplate that is divided into three regions (Panjabi et al., 2001). Model 4 had a superior endplate divided into seven regions (Pitzen et al., 2004). The thickness and region distributions are presented in Figure 10.

The finite element model was constructed with 60697 tetrahedral elements and 13651 nodes. The cortical shell was created with 4552 offset shell elements, less for the model with the removed endplate. The shells of the inferior endplate and the radial cortical shell were set to a half-millimeter thickness and used the same offset shell method. Figure 10 shows how the endplates were sectioned. The cartilaginous endplate was not considered in this analysis

because it is often removed during surgery and does not contribute significantly to the stiffness of the endplates (Polikeit et al., 2003(2)).
Assigned material properties have been previously well documented in literature and are presented in Table 25.

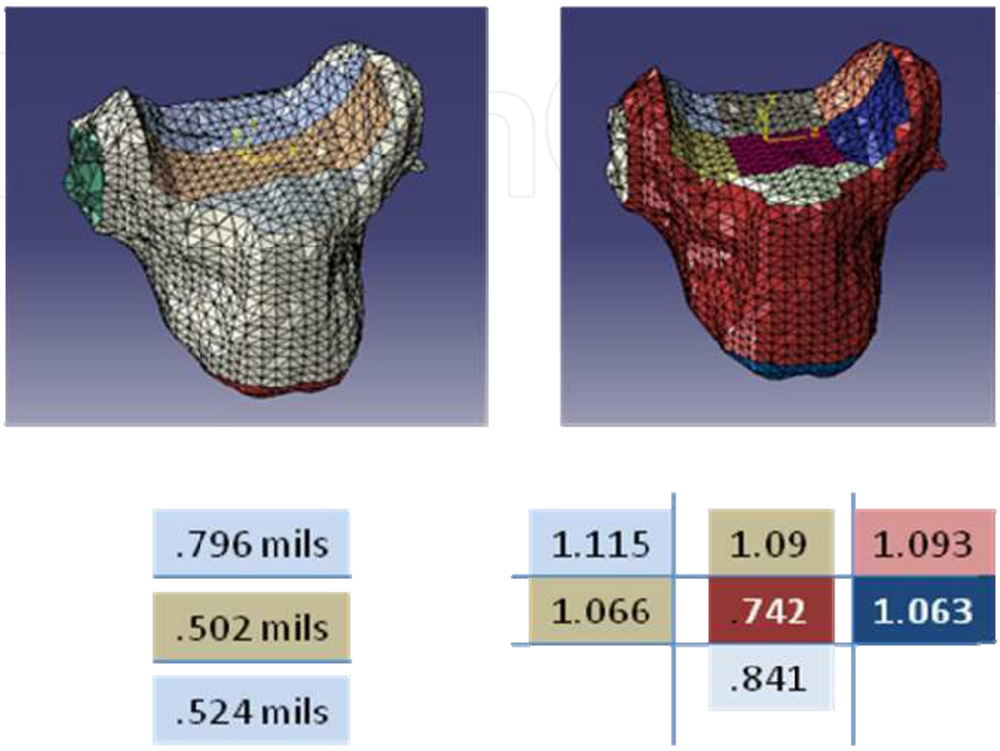

Fig 10. Finite element models of the C3 vertebrae. Left image is Model 3 and the right is Model 4. Below each model is the thickness of the endplate in each region. The thickness regions of the endplate correspond to the colored regions below

	Modulus of Elasticity (MPa)	Poisson's Ratio
Cortical Shell[1]	10,000	.3
Cancellous Core[2]	Ezz = 344, G1,2 = 63	.11
	Eyy = 144, G1,3 = 53	.17
	Exx = 100, G2,3 = 45	.23
Superior Endplate[3,4]	1,000	.3
Inferior Endplate[3,4]	1,000	.3
Posterior Elements[3,4]	3,500	.25

1 – Li and Lewis, 2010
2 - Rohlmann et al., 2006
3 – Polikeit[1] et al., 2003
4 – Polikeit[2] et al., 2003

Table 25. List of material properties applied to the finite element model. This list was compiled from a large group of finite element studies

Material properties were considered to be homogenous. This is not physiologically accurate. The assumption was made that on the macro level the irregularities would be evenly distributed throughout the material sections and represented by the assigned values. The properties were made continuous from point to point and assigned in a hierarchical structure, which separates different bone categories, i.e. cortical and cancellous, into different material groups. This is clinically relevant since the material property definitions simulate bone's various material distributions and can be adapted to replicate disease or injury. The entire vertebra was broken down into posterior elements, cancellous core, radial cortical shell and the superior and inferior endplates. All elements were assigned linear elastic element types. The cancellous core of the vertebral body was assumed to be anisotropic. The axial direction is the strongest due to the difference in cortical bone structure and alignment in the axial direction along lines of stress (Panjabi and White, 1990; Boos and Aebi, 2008).

The models were statically loaded with an axial force of 1000 N and flexion and extension moment of 7.5 Nmm. To avoid the concentration of stress from point loads a pressure distribution was applied to the superior endplate. In this scenario, a higher stress peak develops in the same direction as an applied moment. For example a flexion moment would have a resultant distributed load with a compressive stress peak in the anterior region of the vertebral body. The boundary conditions consisted of fixing the inferior endplate in translation and rotation.

3.3 Results

The results show that the endplate stresses are all approximately the same in magnitude and location. The values of stress calculated in this analytical model are presented in the Table 26 and Figure 11.

	Endplate Flexion (MPa)	**Endplate Extension (Mpa)**	**Percent Diff, Model 1 vs. Model 3,4**	**Core Stress Flexion (Mpa)**	**Core Stress Extension (Mpa)**
Model 1	24.6	25.57	N/A	17.1	34.5
Model 2	N/A	N/A	N/A	74.8	38.2
Model 3	20.7	15.7	17.2, 47.8	13.12	8.5
Model 4	19.5	19.5	22.5, 26.9	20.5	30.14

Table 26. Max stress values in MPa in the core and the endplate from flexion, extension and axial loading

The von Mises stresses range from a minimum of 15.7 MPa, Model 3 in extension, to a maximum of 25.57 MPa, Model 1 in extension. These values are consistent with other studies listed in Table 27. The endplate stresses are also well under the failure stress for cortical bone. The cancellous core stresses are less consistent. A stress range of 8.5 MPa, Model 3 in extension, to 34.5 MPa, Model 1 in extension, was recorded in cases with endplates present. These values are greater than that of the listed failure stress for cancellous bone of 4 MPa, but are in line with some of the previously modeled vertebra in Table 27. In the models with the removed endplate, core stresses reach a maximum of 74.8 MPa, which is much greater than the 4 MPa failure limit.

The von Mises stresses were also analyzed at various depths of the vertebral core. This was done to examine how the stress propagated through the cancellous core. Measurements were taken in 4 spots in the axial plane and at 4 different depths in the sagittal or coronal plane for a total of 16 measurements. The locations of the stress chosen in the axial plane were measured where the stress should have been highest in the cases of flexion and extension. The first set of measurements was taken directly beneath the vertebral endplate. The second set was taken at approximately 1/3 of the height of the vertebral body beneath the superior endplate. The third set was measured at approximately 1/3 of the height of the vertebral body above the inferior endplate. Partial results are presented in the Figure 12 with the complete set of figures in the appendix.

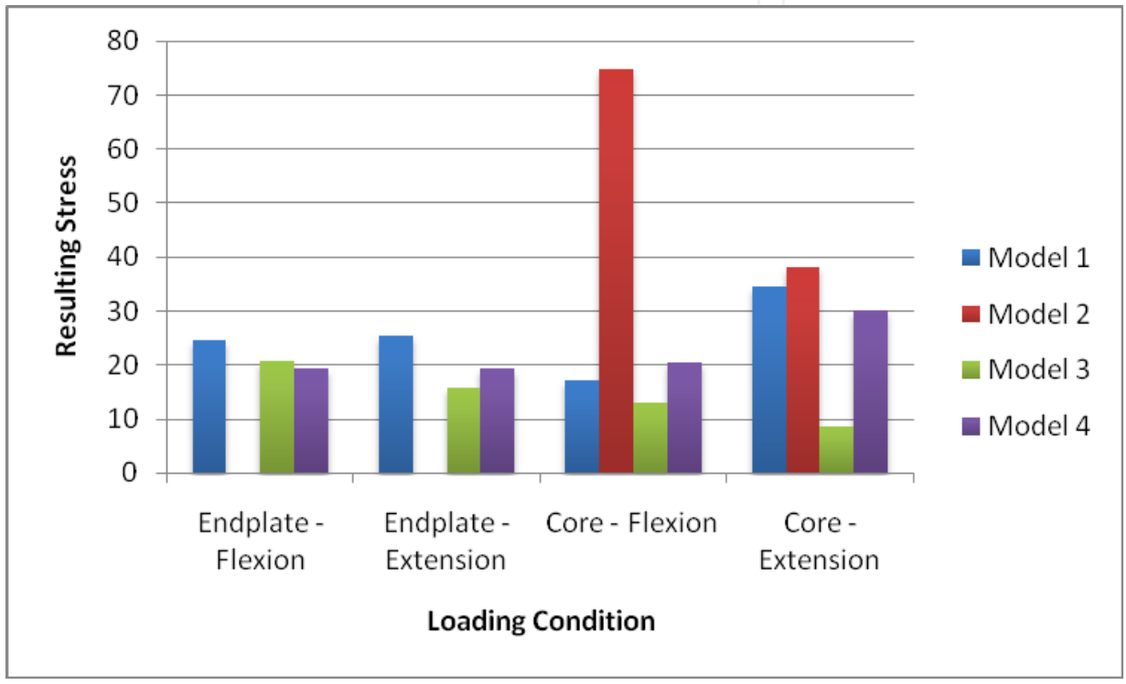

Fig. 11. Stress comparisons between models focusing on endplates and cancellous cores

Researcher	Study Topic	Loads	Max Endplate Stress (MPa)	Max Core Stress (MPa)	Study Level
Galbusera, 2008	Anterior Cervical Fusion	100 N Axial, 2.5 Nmm Bending	2.80	N/A	C5-C6
Denoziere, 2006	Fusion/Mobile Disc	720-1300 N Axial, 11.45 Nmm Axial rotation	90	3.5	L3-L4
Polikeit, 2003	Fusion	1000 N Axial, 12 Nm m Bending	Stress values recorded as percentage increases		L2-L3

Langrana, 2006	Curvature	N/A	40	N/A	L4-L5
Zhang, 2010	Bone Filling Material	400 N Axial, 7.5/3.75 Nmm flex, ext	9.503	.584	L1-L2
Zander, 2002	Bone Graft Location with Fixators	250 N Axial, 7.5 Nmm flex, ext, lat bend	25	N/A	L2-L5
Dai, 1998	Osteoporosis	1200 N Axial, 30 Nmm flex, ext	5.17	24.03	Lumbar
Adams, 2003	Fusion	1310 N Axial	25	N/A	L5

Table 27. The first listed researcher and the emphasis of the study are in columns one and two. The loading condition is in column three and the stress results in the core and endplate are in columns four and five. The level of the spinal column modeled is in column six

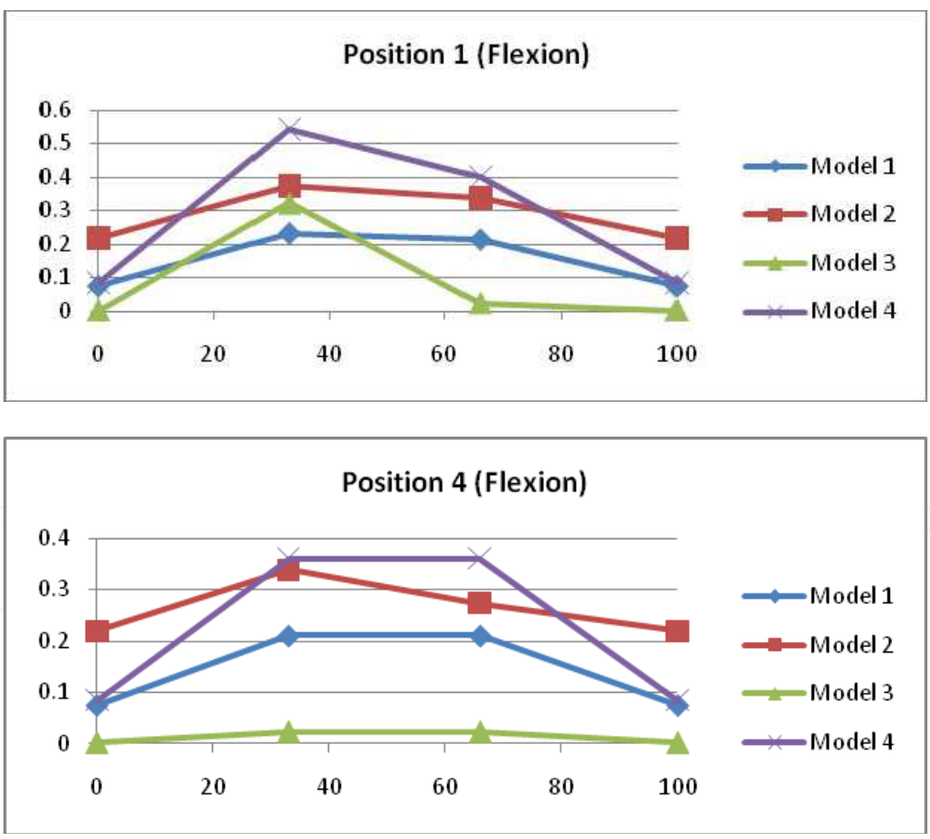

Fig. 12. Each figure represents the cancellous core stress through the height of the vertebral core. The entire chart is present in the appendix. Position 1 is posterior/right, Position 4 is anterior/left. The X-axis represents the percentage of height from top down. The Y-axis is the von Mises stress at each level

The stress results from this test were compared to studies conducted examining the stress in the endplate and vertebral body, and the loads used to obtain these stresses. These results are presented in Table 27. Direct comparisons are difficult because of the wide range of loading conditions, vertebral levels, and different study conditions i.e. fusion, curvature and bone grafts. The results of this study are however within these investigated ranges, which suggest the model is representative of the C3 cervical level.

The differences in reported von Mises stresses can be attributed to different loading conditions and boundary conditions among other things. Few studies go into detail about exactly how loads are applied to finite element models or how the models are bounded. Both factors can have large effects on the outcomes of stress maximums. Research has shown that a stress of 4 MPa is the failure limit for trabecular bone and 131-224 for cortical bone (Linde, 1994; Nigg and Herzog, 1994). These limits can be assumed as a benchmark for the onset of bone failure in the endplates and cancellous core.

The stresses developed in this study indicate that a half-millimeter approximation for the vertebral endplate is adequate. The half-millimeter approximation in Model 1 has a maximum/minimum percent difference from the anthropometric models of 47.8% and 17.2% respectively (percent differences presented in Table 26). The stress generated in Model 1 is also greater than the other models lending to a conservative design if these values are used for mechanical design considerations. The ability to model the endplate with a constant thickness saves time ultimately making the analysis more efficient.

While the endplate stresses were well under its failure limit of 133 MPa the maximum cancellous core stresses in the Model 2 (removed endplate) were much greater than its failure stress of 2 MPa. For example under flexion the core experienced a maximum stress of 74.8 MPa, which is approximately 35 times its failure limit. Subchondral failure was not investigated in this study so its contribution to failure cannot be addresses at this time.

Von Mises values were also recorded through the height of the vertebral core to examine stress propagation. For all cases the 2 MPa core failure stress was not reached except in the case of Model 1, extension, in the posterior right region of the vertebral body where the stress reached 3.98 MPa. This stress is slightly under the upper failure limit of 4 MPa. Table 4 shows average values for stress in each level of the vertebral body under each loading condition: flexion or extension, while also ignoring Model 2 since it does not have an endplate. Table 5 charts stresses associated with flexion and extension in either the posterior or anterior areas of the vertebral core.

Height (as percentage from bottom)	Average von Mises Stress in Flexion (MPa)	Average von Mises Stress in Extension (MPa)
100%	.129	.900 (.620)
66%	.180	.561
33%	.229	.510
0%	.054	.351

Table 28. Average stress propagation through the vertebral body in flexion and extension. The number in parentheses is not considering the highest possibly outlying stress value

Position	Flexion	Extension
1,2	.191	.691
3,4	.105	.467

Table 29. Average stress in the posterior or anterior areas of the vertebral body in flexion and extension. The number in parentheses is not considering the highest possibly outlying stress value

A general trend, in Figure 12, can be seen that the stress is increases towards the center of the vertebral core. In the upper endplate under extension the trend does not hold even if the highest stressed element is not considered. It's likely that there is some load sharing between the endplate and the vertebral core that redistributes load away from the core at the top and bottom near the endplates. The middle the vertebral body seems sufficiently removed from the endplates thus the higher reported stresses. Table 28 also indicates that the posterior of the vertebral body is stressed higher than the anterior portion under both flexion and extension.

3.4 Discussion

Removal of the cortical endplate has a significant effect on the cancellous core stress. Ideally the endplate should be left intact as much as possible. From the evidence above the minimum cancellous core stress was 38.2 MPa. This stress is almost 10 times that of failure limit for cancellous bone using a upper failure limit.

This investigation only analyzes a pressure load that is evenly distributed on the vertebral body. Unless a cage or artificial disc fits perfectly in the disc space with continuous contact, stresses will greatly increase at areas of contact (Adam et al., 2003). Curvature is particularly important in the cervical spine. Unlike the lumbar region that has large flat endplates the cervical spine has a large curvature in the coronal plane that comes from the uncanate processes (Bogduk and Mercer, 2006; Langrana et al., 2006).

The previous analysis shows that a half-millimeter endplate approximation can be used to adequately represent the cortical endplate experimentally. When compared to morphologically complex models the resulting half-millimeter endplate stress was 25.57 MPa and core stresses were 34.5 MPa similar to stresses in other research. It was found that the vertebral body can be modeled analytically without experimentation and can use simplified modeling parameters to save time and cost. Further understanding of regional stress characteristics will be valuable for the design of implantable devices.

4. Appendix

Appendix. Each graph is a specific position in the axial plane of the vertebral body. Position 1 is posterior/right, Position 2 is posterior/left, Position 3 is anterior/right, Position 4 is anterior/left. The X-axis on each chart is the height position in the vertebral body with 100 percent being just under the superior endplate. The Y-Axis is the resulting von Mises stress in MPa.

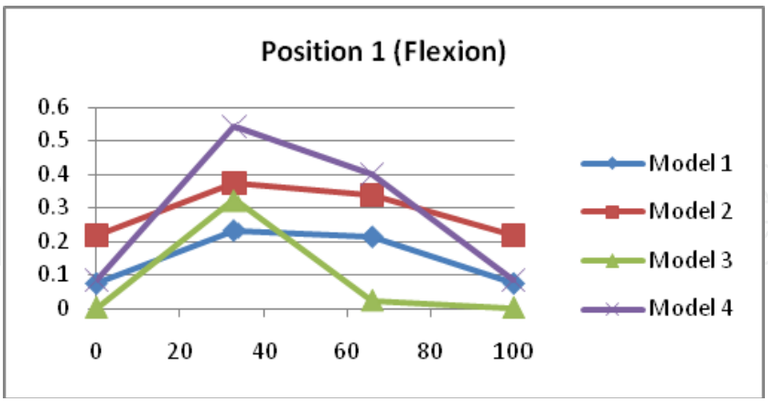
Position 1 (Flexion)
0.6
0.5
0.4
0.3
0.2
0.1
0
0
20
40
60
80
100
Model 1
Model 2
Model 3
Model 4

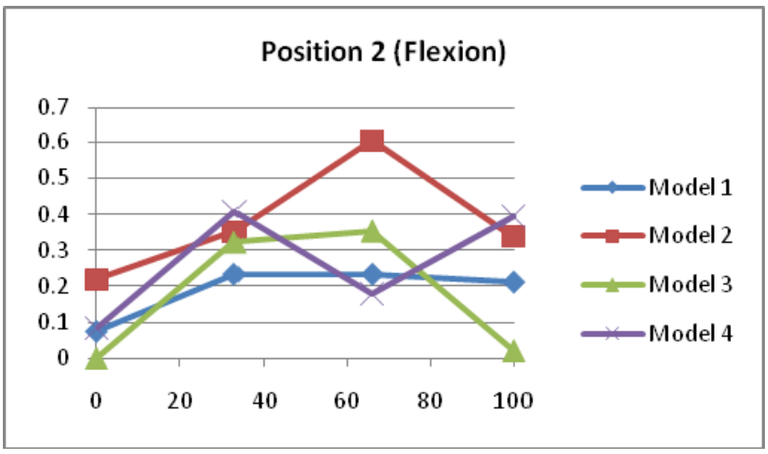
Position 2 (Flexion)
0.7
0.6
0.5
0.4
0.3
0.2
0.1
0
0
20
40
60
80
100
Model 1
Model 2
Model 3
Model 4

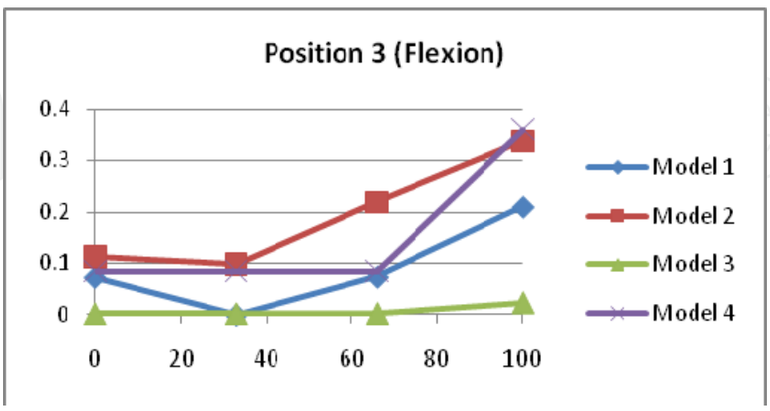
Position 3 (Flexion)
0.4
0.3
0.2
0.1
0
0
20
40
60
80
100
Model 1
Model 2
Model 3
Model 4

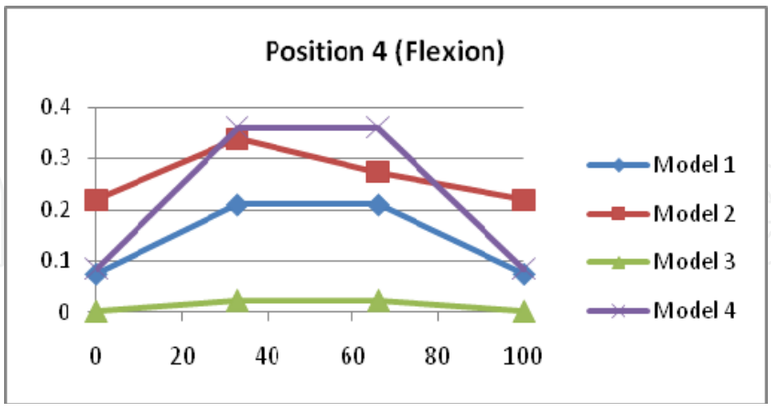
Position 4 (Flexion)
0.4
0.3
0.2
0.1
0
0
20
40
60
80
100
Model 1
Model 2
Model 3
Model 4

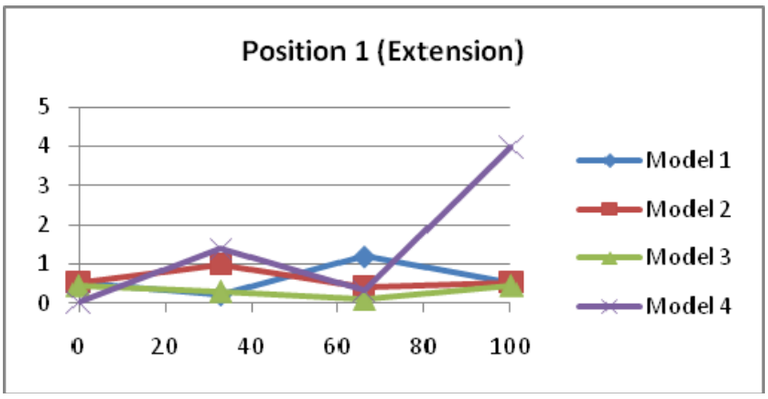
Position 1 (Extension)
5
4
3
2
1
0
0
20
40
60
80
100
Model 1
Model 2
Model 3
Model 4

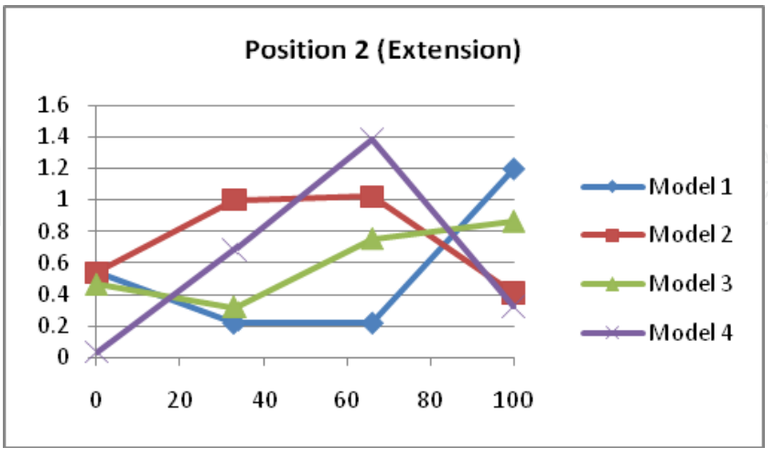
Position 2 (Extension)
1.6
1.4
1.2
1
0.8
0.6
0.4
0.2
0
0
20
40
60
80
100
Model 1
Model 2
Model 3
Model 4

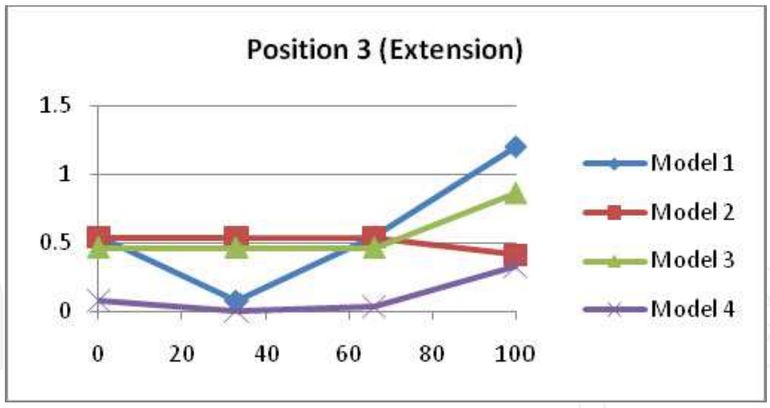

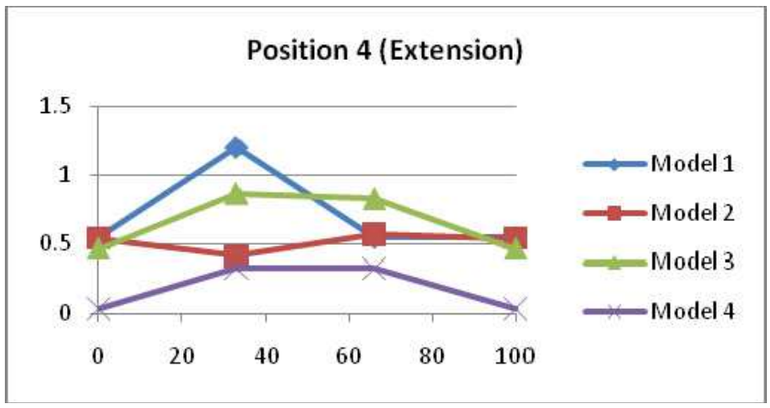

5. Acknowledgments

The authors would like to thank Miami Valley Hospital (Dayton, OH) for support on this project. Specifically Dr. David Udin in the Clinical Research Office, Scott Calvin manager of the Miami Valley Imaging Group, and Matt Binkley fourth year medical student, for assistance in collecting CT images.

6. References

Ambard, D. and Cherblanc, F. (2009) 'Mechanical Behavior of Annulus Fibrosus: A Microstructural Model of Fibers Reorientation', *Annals of Biomedical Engineering*.

Adam, C. Pearcy, M. McCombe, P. 2003. Stress analysis of interbody fusion – Finite element modeling of ineterverteb ral implant and vertebral body. Clinical Biomechanics 18, 265-272

Bogduck, N. and Yoganandan, N. (2001) 'Biomechanics of the cervical spine Part 3: minor injuries', *Clinical Biomechanics*, pp. 267 - 75.

Boos, N., Aebi, M., 2008 Spinal Disorders: Fundamentals of Diagnosis and Treatment. Springer, Zurich, pp. 41-62

Bozic, K.J., Keyak, J.H., Skinner, H.B., Beuff, H.U. and Bradford, D.S. (1994) 'Three-dimensional finite element modeling of a cervical vertebra: An investigation of burst fracture mechanism', *Journal of Spinal Disorders*, pp. 102 - 10.

Bozkus, H.A.K.M.H.M.U.E.B.A.S. (2001) 'Finite element model of the Jefferson fracture: comparison with a cadaver model', *Eur Spine J*, pp. 257-263.

Bozkus, H., Karakas, A., Hanci, M., Uzan, M., Bozdag, E. and Sarioglu, A. (2001) 'Finite element model of the Jefferson fracture: comparison with a cadaver model', *European Spine Journal*, pp. 257-263.

Brolin, K. and Halldin, P. (2004) 'Development of a finite element model of the upper cervical spine and a parameter study of ligament characteristics', *Spine*.

Brolin, K. and Halldin, P. (2004) 'Development of a Finite Element Model of the Upper Cervical Spine and a Parameter Study of Ligament Characteristics', *Spine*, pp. 376-385.

Brolin, K. and Halldin, P. (2005) 'The effect of muscle activation on neck response', *Traffic Injury Prevention*.

Camacho, D.L.A., Nightingale, R.W., Robinette, J.J., Vanguri, S.K., Coates, D.J. and Myers, B.S. (1997) 'Experimetnal flexibility measurements for the development of a computational head-neck model validated for near-vertex head impact', *Proceedings from the 41st Stapp car Crash Conference*, pp. 473 - 486.

Choi, J. Sung, K., 2006. Subsidence after anterior lumbar interbody fusion using paired stand-alone rectangular cages. European Spine Journal 15, 16-22

Dai, L., 1998. The relationship between vertebral body deformity and disc degeneration in lumbar spine of the senile. European Spine Journal 7, 40-44

Denoziere, G. Ku, D., 2006. Biomechanical comparison between fusion of two vertebrae and implantation of an artificial disc. Journal of Biomechanics 39, 766-775

Doherty, B., Heggeness, M. and Esses, S. (1993) 'A biomechanical study of odontoid fractures and fracture fixation', *Spine*, pp. 178 - 84.

Douglas C. Montgomery, a.E.A.P. (1982) *Introduction to Linear Regression Analysis*, New York: John Wiley & Sons, Inc.

Ebara, S., Iatridis, J.C., Setton, L.A., Foster, R.J., Mow, V.C. and Weidenbaum, M. (1996) 'Tensile properties of nondegenerate human lumbar annulus fibrosus', *Spine*, pp. 452 - 61.

Eberlein, R., Holzapfel, G.A. and Froelich, M. (2004) 'Multi-segment FEA of the human lumbar spine including the heterogeneity of the annulus fibrosus', *Computational Mechanics*.

Edwards, W.T. Ferrarra, L.A. Yuan, H.A., 2001. The effect of the vertebral cortex in the thoracolumbar spine. Spine 26, 218-225

Esat, V.L.D.A.M. (2005) 'Combined Multi-Body Dynamic and FE Models of Human Head and Neck', IUTAM Proceedings on Impact Biomechanics, 91-100.

Francis, C.C. (1955) 'Dimensions of the cervical vertebrae', *Anat Rec*, vol. 122, pp. 603-609.

Francis, C.C. (1955) 'Dimensions of the cervical vertebrae', *Anat Rec*, vol. 122, pp. 603-609.

Galbusera, F., Bellini, C.M., Raimondi, M.T., Fornari, M. and Assietti, R. (2008) ' Cervical spine biomechanics following implantation of a disc prosthesis', *Medical Engineering and Physics*, pp. 1127-1133.

Gamst, G., Meyers, L.S. and Guarino, A.J. (2008) *Analysis of Variance Designs: A conceptual and Computational Approach with SPSS and SAS*, New York: Cambridge University Press.

Gilad, I. and Nissan, M. (1986) 'A study of vertebra and disc geometic relations of the human cervical and lumbar spine', *Spine*, pp. 154 - 7.

Glenn Gamst, L.S.M.A.J.G. (2008) *Analysis of Variance Designs: A conceptual and Computational Approach with SPSS and SAS*, New York: Cambridge University Press.

Goel, V.K., Clark, C.R., Harris, K.G. and Schulte, K.R. (1988) 'Kinematics of the cervical spine: effects of multiple total laminectomy and facet wiring', *Jouranl of Orhopaedic Research*, pp. 611 - 19.

Goel, V.K. and Clausen, J.D. (1998) 'Prediction of Load Sharing Among Spinal Components of a C5-C6 Motion Segment Using the Finite Element Approach', *Spine*, pp. 684-691.

Graham, R., Oberlander, E., Stewart, J. and Griffiths, D. (2000) 'Validation and use of a finite element model of C-2 for determination of stress and fracture patterns of anterior odontoid loads', *Journal of Neurosurgery*.

Grant, J. Oxland, T. Dvorak, M., 2001. Mapping the structural properties of the lumbosacral vertebral endplates. Spine 8, 889-896

Greaves, C.Y., Gadala, M.S. and Oxland, T.R. (2008) 'A three-dimensional finite element model of the cervical spine with spinal cord: an investigation of three injury mechanisms', *Annals of Biomedical Engineering*, pp. 396-405.

Ha, S.K. (2006) 'Finite element modeling of multi-level cervical spinal segments (C3-C6) and biomechanical analysis of an elastomer-type prosthetic disc', *Medical Engineering & Physics*, pp. 534-541.

Haghpanahi, M.M.R. (2006) 'Development of a Parametric Finite Element Model of Lower Cervical Spine in Sagital Plane', Proceedings of the 28th IEEE EMBS Annual International Conference, New York City, USA, 1739-1741.

Holzapfel, G.A. (2000) *Nonlinear Solid Mechanics*, New York: Wiley.

Jost, B. et. al., 1998. Compressive strength of interbody cages in the lumbar spine: the eddect of cage shape, posterior instrumentation and bone density. European Spine Journal 7, 132-144

Kallemeyn, N.A., Tadepalli, S.C. and Shivanna, K.H. (2009) ' An interactive multiblock approach to meshing the spine', *Computer Methods and Programs in Biomedicine*, pp. 227-235.

KenethS. Saladin PhD, a.L.M.M.S.N. (2004) *Anatomy & Physiology: The Unity of Form and Function*, Third Ed. edition, New York: McGraw-Hill.

Kulkarni, A. D'Orth Hee, H. Wong, H., 2007. Solis cage (PEEK) for anterior cervical fusion: preliminary radiological results with emphasis on fusion and subsidence. The Spine Journal 7, 205-209

Kumaresan, S., Yoganandan, N. and Pintar, F. (1999) 'Finite Element Analysis of the Cervical Spine: A Material Property Sensitivity Study', *Clinical Biomechanics*, pp. 41-53.

Kumaresan, S., Yoganandan, N., Pintar, F. and Maiman, D. (1999) 'Finite element modeling of the cervical spine: role of intervertebral disc under axial and eccentric loads', *Medical Engineering & Physics*, pp. 689-700.

Kumaresan, S., Yoganandan, N., Pintar, F. and Maiman, D. (1999) 'Finite element modeling of the lower cervical spine: role of intervertebral disc under axial and eccentric loads', *Medical Engineering & Physics*, pp. 689-700.

Kumaresan, S., Yoganandan, N., Pintar, F. and Maiman, D. (1999) 'Finite element modeling of the lower cervical spine: role of intervertebral disc under axial and eccentric loads', *Medical Engineering & Physics*, pp. 689-700.

Kumaresan, S., Yoganandan, N., Pintar, F., Maiman, D. and Kuppa, S. (2000) 'Biomechanical study of pediatric human cervical spine: a finite element approach', *Journal of Biomechanical Engineering*, pp. 60-71.

Kumaresan, S., Yoganandan, N., Voo, L. and Pintar, F. (1998) 'Finite Element Analysis of the Human Lower Cervical Spine', *Journal of Biomechanics*, pp. 87-92.

Langrana, N. Kale, S. Edwards, T. Lee, C. Kopacz, K., 2006. Measurement and analyses of the effects of adjacent

Li, Y. and Lewis, G. (2010) 'Influence of surgical treatment for disc degeneration diseases at C5-C6 on changes in some biomechanical parameters of the cervical spine', *Medical Engineering & Physics*, pp. 593 - 503.

Linde, F., 1994. Elastic and viscoelastic properties of trabecular bone by a compression testing approach. Danish Medical Bulletin 41, 119–138.

Liu YK, C.C.K.K. (1986) 'Quantitative geometry of young human male cervical vertebrae', *Mechanism of Head and Spine Trauma*, pp. 417-431.

Liu, Y.K., Clark, C.R. and Krieger, K.W. (1986) 'Quantitative geometry of young human male cervical vertebrae', *Mechanism of Head and Spine Trauma*, pp. 417-431.

Manohar M. Panjabi, P.J.D.M.V.G.P.T.O.M.a.K.T.M. (1991) 'Cervical Human Vertebrae: Quantitative Three-Dimensional Anatomy of the MIddle and Lower Regions', *Spine*, vol. 16, no. 8, pp. 861-869.

Maurel, N., Lavaste, F. and Skalli, W. (1997) 'A three-dimensional parameterized finite element model of the lower cervical spine. Study of the influence of the posterior articular facets', *Journal of Biomechanics*, pp. 921-931.

Meakin, J. and Huskins, D.W.L. (2001) 'Replacing the nucleus pulposus of the intervertebral disk: prediction of suitable properties of a replacement material using finite element analysis', *Journal of Materials Science*.

Montgomery, D.C. and Peck, E.A. (1982) *Introduction to Linear Regression Analysis*, New York: John Wiley & Sons, Inc.

Moroney, S.P., Schultz, A.B., Miller, J.A.A. and Andersson, G.B.J. (1988) 'Load-displacement properties of lower cervical spine motion segments', *Journal of Biomechanics*, vol. 21, pp. 769-779.

Muller-Gerbl, M. Weiber, S. Linsenmeier, U., 2008. The distribution of mineral density in the cervical vertebral endplates. European Spine Journal 17, 432-438

Nigg, B.M., Herzog, W.H., 1994. Biomechanics of the musculo- skeletal system (Eds.), John Wiley & Sons, Chichester.

Ng, H.-W. and Teo, E.-C. (2001) 'Nonlinear Finite-Element Analysis of the Lower Cervical Spine (C4-C6) Under Axial Loading', *Journal of Spinal Disorders*, pp. 201-10.

Ng, H.-W., Teo, E.-C., Lee, K.-K. and Qiu, T.-X. (2003) 'Finite element analysis of cervical spinal instability under physiologic loading', *Journal of Spinal Disorders & Techniques*, pp. 55 - 63.

Nightingale, R.W., Chancey, V.C., Otaviano, D., Luck, J.F., Tran, L., Prange, M. and Myers, B.S. (n.d) 'Flexion and extension structural properties and strenghts for male cervical spine segments', *Journal of Biomechanics*, pp. 534 - 42.

Nissan M, G.I. (1984) 'The cervical and lumbar vertebrae: An anthropometric model', *Eng Med*, vol. 13, no. 3, pp. 111-114.

Nissan, M. and Gilad, I. (1984) 'The cervical and lumbar vertebrae: An anthropometric model', *Eng Med*, vol. 13, no. 3, pp. 111-114.

Noailly, J., Lacoix, D. and Planell, J.A. (2005) 'Finite element study of a novel intervertebral disc substitute', *Spine*.

Noailly, J., Wilke, H.-J., Planell, J.A. and Lacroix, D. (2007) 'How does the geometry affect the internal biomechanics of a lumbar spine bi-segment finite element model? Consequences on validation process', *Journal of Biomechanics*, pp. 2414-2425.

Ordway, N. Lu, Y. Zhang, X. Cheng, C. Fang. H, Fayyazi, A., 2007. Correlation of the cervical endplate strength with CT measured subchondral bone density. European Spine Journal 16, 2104-2109

Oxland, T.R., 2003. Effects of endplate removal on the structural properties of the lower lumbar vertebral bodies. Spine 8, 771-777

Palomar, A., Calvo, B. and Doblare, M. (2008) 'An accurate finite element model of the cervical spine under quasi-static loading', *Journal of Biomechanics*, pp. 523-531.

Panagiotopoulou, O. (2009) 'Finite element analysis (FEA): applying an engineering method to functional morphology in anthropology and human biology', *Annals of Human Biology*, pp. 609 - 23.

Panjabi, M., White. A., 1990. Clinical Biomechanics of the Spine. Lippencott, Philidelphia

Panjabi, M. Chen, M.C. Wang, J.L., 2001. The cortical architecture of the human cervical vertebral bodies. Spine 22, 2478-2484

Panjabi, M.M., Crisco, J.J., Vasavada, A., Oda, T., Cholewicki, J., Nibu, K. and Shin, E. (2001) 'Mechanical properties of the human cervical spine as shown by three-dimensional load-displacement curves', *Spine*, pp. 2692 - 2700.

Panjabi, M., Duranceau, J., Goel, V., Oxland, T. and Takata, K. (1991) 'Cervical human vertebrae. Quanatative three-dimensional anatomy of the middle and lower regions', *Spine*, pp. 861 - 9.

Panjabi, M.M., Duranceau, J., Goel, V., Oxland, T. and Takata, K. (1991) 'Cervical Human Vertebrae: Quantitative Three-Dimensional Anatomy of the MIddle and Lower Regions', *Spine*, vol. 16, no. 8, pp. 861-869.

Panzer, M.B. and Cronin, D.S. (2009) 'C4-C5 segment finite element model development, validation, and load-sharing investigation', *Journal of Biomechanics*, pp. 480-490.

Pintar, F., Yoganandan, N., Pesigan, M., Reinartz, J., Sances, A. and Cusick, J. (1995) 'Cervical vertebral strain measurements under axial and eccentric loading', *Journal of Biomechanical Engineering*, pp. 474 - 8.

Pintar, F.A., Yoganandan, N., Pesigan, M., Reinartz, J., Sances, A. and Cusick, J.F. (1995) 'Cervical vertebral strain measurements under axial and eccentricl loading', *Journal of Biomechanical Engineering*, pp. 474 - 8.

Pitzen, T., Geisler, F., Matthis, D., Muller-Storz, H., Barbier, D., Steudel, W.-I. and Feldges, A. (2002) 'A finite element model for predicting the biomechanical behaviour of the human lumbar spine.', *Control Engineering Practice*, pp. 83-90.

Pitzen, T., Geisler, F.H., Matthis, D., Muller-Storz, H., Pedersen, K. and Steudel, W.-I. (2001) 'The influence of cancellous bone density on load sharing in human lumbar spine: a comparison between an intact and a surgically altered motion segment', *European Spine Journal*, pp. 23-29.

Pitzen, T., Matthis, D. and Steudel, W.-I. (2002) 'Posterior Element Injury and Cervical Spine Flexibility Following Anterior Cervical Fusion and Plating', *European Journal of Trauma*, pp. 24-30.

Pitzen, T. et. al., 2004. Variation of endplate thickness. European Spine Journal 13, 235-240

Polikeit[1], A. et. al., 2003. Factors influencing stresses in the lumbar spine after the insertion of intervertebral cages: Finite element analysis. European Spine Journal 12, 413-420

Polikeit[2], A. et. al., 2003. The importance of the endplate for interbody cages in the lumbar spine. European Spine Journal 12, 556-561

Richter, M., Wilke, H.J., Kluger, P., Claes, L. and Puhl, W. (2000) 'Load-displacement properties of the normal and injured lower cervical spine in vitro', *European Spine Journal*, pp. 104 - 8.

Rohlmann, A. Zander, T. Bergmann, G., 2006. Effects of fusion-bone stiffness on the mechanical behavior of the lumbar spine after vertebral body replacement. Clinical Biomechanics 21, 221-227

S.H. Tan, E.C.T.a.H.C.C. (2004) 'Quantitative three-dimensional anatomy of cervical, thoracic and lumbar vertebrae of Chinese Singaporeans', *European Spine Journal*, vol. 13, pp. 137-146.

Sairyo, K., Goel, V.K., Masuda, A., Vishnubhotla, S., Faizan, A., Biyani, A., Ebraheim, N. and Yonekura, D.e.a. (2006) ' Three-dimensional finite element analysis of the pediatric lumbar spine. Part 1: pathomechanism of apophyseal bony ring fracture', *European Spine Journal*, pp. 923-929.

Sairyo, K., Goel, V.K., Masuda, A., Vishnubhotla, S., Faizan, A., Biyani, A., Ebraheim, N. and Yonekura, D.e.a. (2006) 'Three-dimensional finite element analysis of the pediatric lumbar spine. Part II: biomechanical change as the initiating factor for pediatric ishmic spondylolisthesis after growth plate', *European Spine Journal*, pp. 930-935.

Sairyo, K., Goel, V.K., Masuda, A., Vishnubhotla, S., Faizan, A., Biyani, A., Ebraheim, N. and Yonekura, D.e.a. (206) ' Three-dimensional finite element analysis of the pediatric lumbar spine. Part II: biomechanical change as the initiating factor for pediatric ishmic spondylolisthesis after growth plate', *European Spine Journal*, pp. 930-935.

Saladin, K.S. and Miller, L. (2004) *Anatomy & Physiology: The Unity of Form and Function*, Third Ed. edition, New York: McGraw-Hill.

Schmidt, H.H.F.D.J.K.Z.C.L.W.H. (2007) 'Application of a calibration method provides more realistic results for a finite element model of a lumbar spinal segment', *Clinical Biomechanics*, pp. 377-384.

Shirazi-Adl, A. (2006) ' Analysis of large compression loads on lumbar spine in flexion and in torsion using a novel wrapping element.', *Journal of Biomechanics*, pp. 267-275.

Stemper, B.D., Yoganandan, N., Pintar, F.A. and Rao, R.D. (2006) 'Anterior longitudinal ligament injuries in whiplash may lead to cervical instability', *Medical Engineering & Physics*.

Tan, S.H., Teo, E.C. and Chua, H.C. (2004) 'Quantitative three-dimensional anatomy of cervical, thoracic and lumbar vertebrae of Chinese Singaporeans', *European Spine Journal*, vol. 13, pp. 137-146.

Teo, J.C.M., Chui, C.K., Wang, Z.L., Ong, S.H., Yan, C.H., Wang, S.C., Wong, H.K. and Teoh, S.H. (2007) 'Heterogenous meshing and biomechanical modeling of human spine.', *Medical Engineering and Physics*, pp. 277-290.

Teo, E.C. and Ng, H.W. (2001) 'Evaluation of the role of ligaments, facets and disc nucleus in lower cervical spine under compression and sagittal moments using finite element method', *Medical Engineering & Physics*, pp. 155 - 64.

Teo, E.C. and Ng, H.W. (2001) 'First cervical vertebra (atlas) fracture mechanism studies using finite element method', *Journal of Biomechanics*, pp. 13-21.

Traynelis, P.A., Donaher, R.M., Roach, R.M. and Goel, v.K. (1993) 'Biomechanical comparison of anterior caspar plate and three-level posterior fixation techniques in human cadaveric model', *Journal of Neurosurgery*, pp. 96 - 103.

Van Jonbrgen, H.P. Spruit, M. Anderson, P. Pavlov, P., 2005. Anterior cervical interbody fusion with a titanium box cage: early radiological assessment of fusion and subsidence. The Spine Journal 5, 645-649

Voo, L.M., Kumaresan, S., Yoganandan, N., Pintar, F. and Cusick, J.F. (1997) 'Finite element analysis of cervical facetectomy', *Spine*.

Wheeldon, J.A., Pintar, F.A., Knowles, S. and Yoganandan, N. (2006) 'Experimental flexion/extension data corridors for validation of finite element models of the young, normal cervical spine', *Journal of Biomechanics*, pp. 375 - 80.

Wheeldon, J.A., Stempter, B.D., Yoganandan, N. and Pintar, F.A. (2008) 'Validation of finite element model of the young normal lower cervical spine', *Annals of Biomedical Engineering*, pp. 1458-1469.

Yoganandan, N., Kumaresan, S. and Pintar, F.A. (2000) 'Geometric and mechanical properties of human cervical spine ligaments', *Journal of Biomechanical Engineering*, pp. 623 - 29.

Yoganandan, N., Kumaresan, S. and Pintar, F.A. (2001) 'Biomechanics of the cervical spine part 2. Cervical spine soft tissue responses and biomechanical modeling', *Clinicals Biomechanics*, pp. 1-27.

Yoganandan, N., Kumaresan, S., Voo, L. and Pintar, F.A. (1996) 'Finite elemnt applications in human cervical spine modeling', *Spine*.

Yoganandan, N., Kumaresan, S., Voo, L. and Pintar, F.A. (1997) 'Finite Element Model of the Human Lower Cervical Spine: Parametric Analysis of the C4-C6 Unit', *Journal of Biomechanical Engineering*, pp. 81-92.

Yoganandan, N., Kumaresan, S., Voo, L., Pintar, F. and Larson, S. (1996) 'Finite Element Analysis of the C4-C6 Cervical Spine Unit', *Medical Engineering & Physics*, pp. 569-574.

Zander, T. Rohlmann, A. Klockner, C. Bergmann, G., 2002. Effect of bone graft characteristics on the mechanical behavior of the lumbar spine. Journal of Biomechanics 35, 491-497

Zhang, Q.H., Teo, E.C., Ng, H.W. and Lee, V.S. (2006) 'Finite element analysis of moment-rotation relationships for human cervical spine', *Journal of Biomechanics*.

Zheng, P.D..N., Young-Hing, M.D..K. and Watson, P.D..L.G. (2000) 'Morphological and biomechanical studies of pedicle screw fixation for the lower cervical spine', *Journal of Systems Integration*, pp. 55-66.

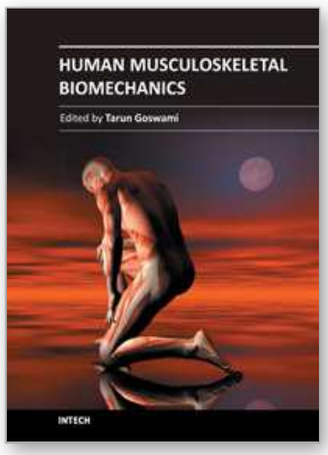

Human Musculoskeletal Biomechanics

Edited by Dr. Tarun Goswami

ISBN 978-953-307-638-6
Hard cover, 244 pages
Publisher InTech
Published online 05, January, 2012
Published in print edition January, 2012

This book covers many aspects of human musculoskeletal biomechanics. As the title represents, aspects of forces, motion, kinetics, kinematics, deformation, stress, and strain are examined for a range of topics such as human muscles, skeleton, and vascular biomechanics independently or in the presence of devices. Topics range from image processing to interpret range of motion and/or diseases, to subject specific temporomandibular joint, spinal units, braces to control scoliosis, hand functions, spine anthropometric analyses along with finite element analyses. Therefore, this book will be valuable to students at introductory level to researchers at MS and PhD level searching for science of specific muscle/vascular to skeletal biomechanics. This book will be an ideal text to keep for graduate students in biomedical engineering since it is available for free, students may want to make use of this opportunity. Those that are interested to participate in the future edition of this book, on the same topic, as a contributor please feel free to contact the author.

How to reference

In order to correctly reference this scholarly work, feel free to copy and paste the following:

Susan Hueston, Mbulelo Makola, Isaac Mabe and Tarun Goswami (2012). Cervical Spine Anthropometric and Finite Element Biomechanical Analysis, Human Musculoskeletal Biomechanics, Dr. Tarun Goswami (Ed.), ISBN: 978-953-307-638-6, InTech, Available from: http://www.intechopen.com/books/human-musculoskeletal-biomechanics/cervical-spine-anthropometric-and-finite-element-biomechanical-analysis

INTECH
open science | open minds

InTech Europe
University Campus STeP Ri
Slavka Krautzeka 83/A
51000 Rijeka, Croatia
Phone: +385 (51) 770 447
Fax: +385 (51) 686 166
www.intechopen.com

InTech China
Unit 405, Office Block, Hotel Equatorial Shanghai
No.65, Yan An Road (West), Shanghai, 200040, China
中国上海市延安西路65号上海国际贵都大饭店办公楼405单元
Phone: +86-21-62489820
Fax: +86-21-62489821

IntechOpen